

Ball-map : Homeomorphism between compatible surfaces

GVU Technical Report Number :
GIT-GVU-06-05

Frédéric Chazal¹
Mathematics Institute
of Burgundy

André Lieutier²
Dassault Systèmes
(Aix-en- Provence)
and LMC/IMAG

Jarek Rossignac³
Georgia Institute of Technology

Brian Whited⁴
Georgia Institute of Technology

February 4, 2006

¹e-mail: fchazal@u-bourgogne.fr

²e-mail: andre.lieutier@ds-fr.com

³e-mail: jarek@cc.gatech.edu

⁴e-mail: fender@cc.gatech.edu

Contents

| | | |
|----------|--|-----------|
| 1 | The Ball map | 1 |
| 1.1 | Introduction | 1 |
| 1.2 | Background concepts and definitions | 3 |
| 1.2.1 | Compact connected $(n - 1)$ -manifolds embedded in R^n | 3 |
| 1.2.2 | Mean feature size and smoothness | 3 |
| 1.2.3 | Comparing two $(n - 1)$ -manifolds embedded in R^n | 5 |
| 1.2.4 | Moat and median | 6 |
| 1.3 | Ball-compatibility and ball-map | 6 |
| 2 | ball-compatibility | 9 |
| 2.1 | Conditions for ball-compatibility | 9 |
| 2.1.1 | Necessary and sufficient condition for C^1 manifolds | 9 |
| 2.1.2 | A sufficient condition relying on Hausdorff distance | 12 |
| 2.2 | Bounding Fréchet distance | 14 |
| 3 | Properties of the Ball map | 16 |
| 3.1 | Smoothness | 16 |
| 3.1.1 | The smoothness of the ball-map | 16 |
| 3.1.2 | Smoothness of the median surface | 18 |
| 3.2 | Ball-map surface encoding | 19 |
| 3.3 | Implementation | 21 |
| 3.3.1 | Piecewise-circular curves | 21 |
| 3.3.2 | Triangle-mesh approximations | 22 |
| 4 | The conformal point of view | 23 |
| 4.1 | Ball-map and conformal invariance | 23 |
| 4.1.1 | Conformal group | 23 |
| 4.1.2 | Generalizing ball-map | 24 |
| 4.2 | Ball-map and isotopy | 28 |
| 4.2.1 | Broken line morph isotopy | 28 |
| 4.2.2 | Circular arc morph isotopy | 28 |
| 5 | Anticipated applications | 31 |
| 6 | Conclusion | 35 |

Abstract

Homeomorphisms between curves and between surfaces are fundamental to many applications of 3D modeling, graphics, and animation. They define how to map a texture from one object to another, how to morph between two shapes, and how to measure the discrepancy between shapes or the variability in a class of shapes. Previously proposed maps between two surfaces, S and S' , suffer from two drawbacks: (1) it is difficult to formally define a relation between S and S' which guarantees that the map will be bijective and (2) mapping a point x of S to a point x' of S' and then mapping x' back to S does in general not yield x , making the map asymmetric. We propose a new map, called ball-map, that is symmetric. We define simple and precise conditions for it to be a homeomorphism. We show that these conditions apply when the minimum feature size of each surface exceeds their Hausdorff distance. The ball-map, $\text{BM}_{S,S'}$, between two such manifolds, S and S' , maps each point x of S to a point $x' = \text{BM}_{S,S'}(x)$ of S' . $\text{BM}_{S',S}$ is the inverse of $\text{BM}_{S,S'}$, hence BM is symmetric. We also show that, when S and S' are C^k $(n-1)$ -manifolds in R^n , $\text{BM}_{S,S'}$ is a C^{k-1} diffeomorphism and defines an C^{k-1} ambient isotopy that smoothly morphs between S to S' . In practice, the ball-map yields an excellent map for transferring parameterizations and textures between ball compatible curves or surfaces. Furthermore, it may be used to define a morph, during which each point x of S travels to the corresponding point x' of S' along a circular arc that is normal to S at x and to S' at x' .

Chapter 1

The Ball map

1.1 Introduction

Many problems in 3D graphics, animation, and data analysis require building a map between two curves or between two surfaces [13][25][9]. Such a map may be used to transfer a texture from a surface S to a simplified version S' of S [28] or to formulate the discrepancy between S and S' , [6] [21] [26] better than it has been possible so far by using variations of the Hausdorff distance [18] [20]. Finally, it provides a point-to-point association for computing 3D morphs [1] [15].

In most cases, a bijective map (homeomorphism) is desired. Several maps have been used in the past. The closest-point map $C_{S',S} : S' \rightarrow S$ maps a point x' of S' to its closest point $x = C_{S',S}(x')$ of S . Its inverse, the orthomap [12] $O_{S,S'} : S \rightarrow S'$ maps a point x of S to the point x' of S' that is the first intersection of a ray starting from x along the normal to S at x oriented towards the interior of the symmetric difference between the regions bounded by S and S' . According to [8], the orthomap and the closest-point map from S to S' are homeomorphisms if the minimum feature sizes of S and S' both exceed $h/(2 - \sqrt{2})$, where h is the Hausdorff distance between S and S' . We refer to this condition as the normal-compatibility condition between two surfaces in 3D or curves in 2D. Unfortunately, the orthomap and its inverse are not symmetric, and thus, in a sense, suboptimal [13]. In particular, if x' is the closest point on S' to a point x of S ,

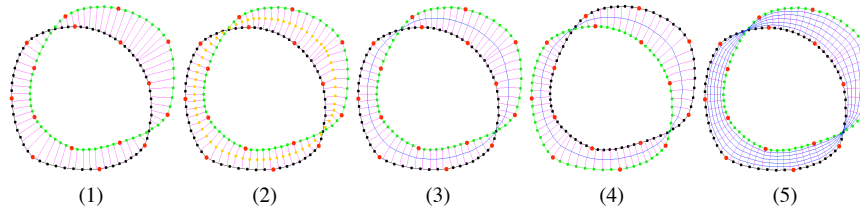


Figure 1.1: The ball morph between two curves S and S' may be performed using straight line trajectory from each green point x of S to the corresponding point x' of S' (figure 1), a broken line trajectory going through point c of the middle set (figure 2), or a circular arc approaching both curves orthogonally (figure 3). Arcs (figure 4) computed from the reverse ball-map from S' to S are consistent with the ball-map from S to S' . Several key-frames of the morph animation are shown in blue (figure 5).

x is not in general the closest point on S to x' . Hence, one anticipates the existence of a better map producing a shorter average distance between points x of S and their image on S' .

In this paper, we propose a new map, which we named *ball-map*, between any two $(n-1)$ -manifolds in R^n . We show that under specific conditions, the two manifolds are, what we call, ball-compatible and the ball-map $\text{BM}_{S,S'} : S \rightarrow S'$ from the manifold S onto the manifold S' is a homeomorphism and $\text{BM}_{S,S'}$ is the inverse of $\text{BM}_{S',S}$. Furthermore, we show that the ball-map defines a smooth isotopy through which S may morph into S' (Fig. 1.1). We show that a sufficient condition for the ball-map to be an homeomorphism is that the minimum feature sizes of S and S' both exceed h , where h is the Hausdorff distance between S and S' . We say that curves or surfaces satisfying this condition are minimum feature compatible. Note that this sufficient feature-respecting compatibility condition ensuring ball-compatibility is less restrictive than the corresponding condition for normal-compatibility, which requires a tighter ratio of $h/(2-\sqrt{2})$.

Minimum-feature compatibility is an optimal condition for the equality of the Hausdorff and Fréchet distances and provides a mild condition for surface isotopy. Consequently, we anticipate that the ball-map will be of value for comparing smooth surfaces and for formulating the error between a shape and its approximation that ensures topological compatibility. In solid modeling, the ball-map will make it possible to simplify the expression of the discrepancy between a CAD model of a nominal part and 3D measurements of manufactured products. In particular, it provides a generalized and constructive version of the theorem proven in [3] that uses metric conditions to *guarantee surface isotopy*.

Finally, it follows from the definition of the ball-map that it is a conformal invariant (i.e. invariant under Möbius transforms). Note that the closest-point projection is invariant under isometries only.

When the discrepancy between the two surfaces or the two curves exceeds the feature-respecting compatibility condition, the ball-map may not be a homeomorphism. In such cases, one may need to rely on more general, and less precise, mappings [9]. Still, even in such incompatible cases, the ball-map may be of use for automatically generating, an optimal map and morph between consecutive frames in a family that samples the morph between disparate curves or surfaces.

The remainder of this paper is organized as follows. Section 1.2 provides preliminary definitions and assumptions used throughout the rest of the paper. In section 1.3, we introduce the ball-compatibility and prove the continuity of the ball-map. Section 2.1 provides a necessary and sufficient condition for C^1 manifolds to be ball-compatible and then a sufficient feature-respecting compatibility condition formulated in terms of the Hausdorff distance. We show in section 2.2 that for a pair of surfaces satisfying the feature-respecting compatibility condition the Fréchet distance equals the Hausdorff distance. Section 3.1 relates the smoothness of the ball-map and of the median surface that it defines to the smoothness of the two ball compatible surfaces. Section 3.2 consider, being given a surface S , the expression of a ball-compatible surface S' by the field of radius: $\rho : S \rightarrow \mathbb{R}$ that associates to a point $x \in S$ the radius of the ball tangent to S at x and to S' at $x' = \text{BM}_{S,S'}(x)$. Section 3.3 sketches two implementations for the automatic computation of the ball-map: one for smooth piecewise-circular curves in 2D and one for triangle-mesh approximations of smooth surfaces in 3D. In section 4.1 we investigate in more detail the conformal invariance of the ball-map, we propose an extension of the ball-map that coincide with the classical stereographic projection between spheres and planes. We show in section 4.2 that the ball-map is not only a

homeomorphism, but in fact an isotopy. The sufficient condition for ball-map is then a metric based sufficient condition for two manifolds to be isotopic. Section 5 reviews the anticipated impact of the new results developed in this paper on practical applications. Finally section 6 concludes and mentions possible extensions and future work.

1.2 Background concepts and definitions

For any set X , \bar{X} , X° , ∂X and X^c denote respectively the closure, the interior, the boundary and the complement of X .

1.2.1 Compact connected $(n - 1)$ -manifolds embedded in R^n

We consider here a $(n - 1)$ -manifold S embedded in R^n . Hence, each one of its points has a neighborhood homeomorphic to an $(n - 1)$ -dimensional disk [27]. For example, it may be a curve embedded in R^2 or a surface embedded in R^3 . When the $(n - 1)$ -manifold S is orientable and smooth, a unit-length normal vector field to S defines a map $\vec{n} : x \rightarrow \vec{n}(x)$ known as the Gauss map.

A compact connected $(n - 1)$ -manifold S embedded in R^n is orientable and the complement of S in R^n has two connected components ([10] pp. 234). In other words, S decomposes R^n into three connected parts: S itself, S_i , the interior, and S_e , the exterior. S_e is the unbounded part of the complement of S . Note that S_i and S_e are open. Using Computer Aided Design terminology, in two dimensions S would be a closed curve separating the interior face S_i from the unbounded exterior face S_e . In three dimensions, S would be a single shell surface without borders, although possibly with handles.

The *cut* $C(S)$ of S is the *medial axis* of S^c . It is the set of points (of S^c) that have at least two closest points on S . From [16], we know that $C(S)$ has exactly one connected component in S_i , that we denote $C_i(S)$ and may have one or more connected components in S_e that we denote $C_e(S)$. From the definition we have of course: $C(S) = C_i(S) \cup C_e(S)$. The *local feature size* [17], or *lfs*, is defined for each point $x \in S$ as the distance to $C(S)$: $\text{lfs}(x) = \inf_{y \in C(S)} d(x, y)$.

The *minimal feature size* or *mfs* is the infimum of the values of *lfs* on S :

$$\text{mfs}(S) = \inf_{x \in S} \text{lfs}(x) = \inf_{x \in S, y \in C(S)} d(x, y)$$

the concept of *mfs* has been introduced by Federer in the 50's and called *reach*.

1.2.2 Mean feature size and smoothness

The ball-map is not a homeomorphism when the curves or surfaces considered exhibit sharp features, i.e., points with unbounded curvature. To preclude these, we could simply require that each surface S for which the ball-map is defined be C^2 , by which we mean that it has a *continuous* curvature. Unfortunately, the boundary of a solid in which the sharp edges have been rounded by smooth fillets or blends [22] will have bounded curvature, but its boundary may not be C^2 . Since we wish to extend the results discussed here to such shapes, which are common in practices, we need a less constraining characterization of smoothness.

Note that, in the Computer Aided Geometric Design terminology, a distinction has been introduced between C^k and G^k (" G " for Geometric) continuity. However, this distinction does not apply here because we are using the classical terminology of differential

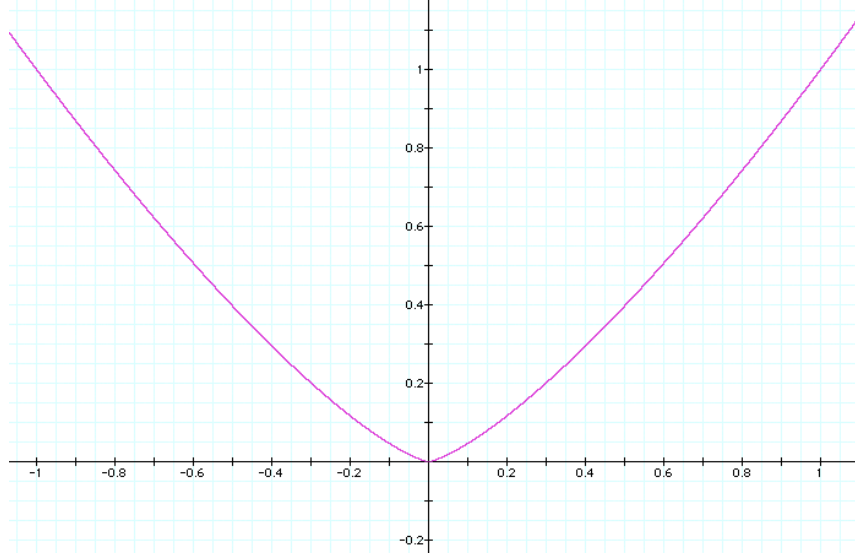


Figure 1.2: $\mathcal{C} = \{(x, y) \mid x^4 - y^3 = 0\}$ is a C^1 curve with $\text{mfs}(\mathcal{C}) = 0$. Its cut, medial axis of its complement, is $C(\mathcal{C}) = \{(0, y) \mid y > 0\}$.

geometry, where a C^k manifold is one that admits a local regular C^k parameterization which corresponds to the G^k continuity notion used by the CAGD community. (The term *regular* means here: "whose derivative has full rank everywhere".)

Requiring only that the surfaces be C^1 is insufficient, since it does not guarantee that the curvature is bounded. As an example, consider the curve (see figure 1.2) defined by:

$$\mathcal{C} = \{(x, y) \in \mathbb{R}^2 : y^3 - x^4 = 0\} = \{(x, y) \in \mathbb{R}^2 : y = |x|^{\frac{4}{3}}\}$$

The curve \mathcal{C} is C^1 , but $\text{mfs}(\mathcal{C}) = 0$. Indeed, considering the first derivative of $x \mapsto |x|^{\frac{4}{3}}$, one observes that the curve \mathcal{C} admits the line $y = 0$ as tangent line at point $(0, 0)$, while the second derivative, being not bounded near the point $(0, 0)$, tells us that the curvature is not bounded near this point and the medial axis is at distance 0 from the point $(0, 0)$. Hence, we need a compromise, or a more precise definition of smoothness. From now on, we assume that all surfaces and curves are compact manifolds satisfying $\text{mfs}(S) > 0$.

For compact manifolds, the condition $\text{mfs}(S) > 0$ is equivalent to the $C^{1,1}$ property, which means that the two surfaces are C^1 manifolds with a Lipschitz condition on the surface normals. This condition may be explained as follows. Let d_S denote the *geodesic distance* on S , that is, for $x_1, x_2 \in S$, $d_S(x_1, x_2)$ is the length of the shortest path from x_1 to x_2 on S . The *Lipschitz condition* on the Gauss map \vec{n}_S can be expressed as:

$$\|\vec{n}_S(x_2) - \vec{n}_S(x_1)\| \leq \frac{1}{\text{mfs}(S)} d_S(x_1, x_2) \quad (1.1)$$

1.2.3 Comparing two $(n - 1)$ -manifolds embedded in R^n

We consider two compact, connected $(n - 1)$ -manifolds S and S' embedded in R^n . The discrepancy between two such manifolds may be measured in a variety of ways. In this paper we consider both Hausdorff and Fréchet distances.

Definition 1.2.1 (Hausdorff distance) Let A and B be two compact subsets of \mathbb{R}^n . The Hausdorff distance between A and B is defined by

$$d_H(A, B) = \max \left(\sup_{x \in A} d(x, B), \sup_{y \in B} d(y, A) \right)$$

The Hausdorff distance $d_H(A, B)$ between two compact sets A and B may also be defined in terms of r -thickening. The r -thickening A^r of A is the union of all open balls of radius r and center on A . Note that A^r is the Minkowski sum of A with an open ball of radius r and center at the origin. The r -thickening operator was used as a tool for offsetting, rounding and filleting operations [23] and for shape simplification [14]. The Hausdorff distance, $d_H(A, B)$, between two sets A and B is the infimum of the radius r such that $A \subset B^r$ and $B \subset A^r$. The Hausdorff distance defines a distance on the space of compact subsets of \mathbb{R}^n : $d_H(A, B) = 0 \Rightarrow A = B$, $d_H(A, B) = d_H(B, A)$ and $d_H(A, C) \leq d_H(A, B) + d_H(B, C)$ (see [2]).

We recall that a *homeomorphism* is a continuous bijection, the inverse of which is also continuous. We say that two sets are homeomorphic if there exists a homeomorphism between them: in this case they are identical regarding intrinsic topological properties. Hausdorff distance allows us to measure the discrepancy between any two compact sets, even when they are not homeomorphic. When one wants to measure the discrepancy between two homeomorphic compact sets A and B , the Hausdorff distance does not provide any information about how far one has to move points of A to B in order to realize a homeomorphism. In other words, two compact sets A and B may have a very small Hausdorff distance yet any homeomorphism between them will map at least some distant pairs (see figure 1.3). So instead of considering the Hausdorff distance, it may be more relevant for homeomorphic shapes to consider the Fréchet distance as a discrepancy measure.

Definition 1.2.2 (Fréchet distance) Let S and S' be two compact homeomorphic submanifolds of \mathbb{R}^n . Let $\mathcal{F} = \{f : S \rightarrow S' : f \text{ is an homeomorphism}\}$ be the set of all homeomorphisms between S and S' . Given such a homeomorphism f , $\sup_{x \in S} d(x, f(x))$ is the maximum displacement of the points of S by f . The Fréchet distance between S and S' is the infimum of this maximum displacement among all the homeomorphisms. It is defined by

$$d_F(S, S') = \inf_{f \in \mathcal{F}} \sup_{x \in S} d(x, f(x)).$$

It is a classical exercise to check that the Fréchet distance satisfies the properties defining a distance and that one always has

$$d_H(S, S') \leq d_F(S, S').$$

In general, the Fréchet distance is more difficult to compute than the Hausdorff distance since one has to find an infimum among all the homeomorphisms between S and S' . In section 2.2, we show that, under specific conditions (theorem 2.2.1), the Hausdorff and Fréchet distances are equal.

When a homeomorphism and its inverse are both C^k -smooth, the homeomorphism is a C^k -*diffeomorphism*. If a homeomorphism may be realized by a continuous deformation, it defines an *isotopy*:

Definition 1.2.3 (Isotopy and ambient isotopy) An isotopy between S and S' is a continuous map $F : S \times [0, 1] \rightarrow \mathbb{R}^n$ such that $F(\cdot, 0)$ is the identity of S , $F(S, 1) = S'$, and

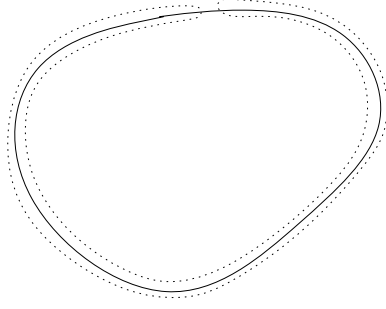


Figure 1.3: The curves in solid and dotted line are close to each other in terms of the Hausdorff distance, while they are significantly different in terms of the Fréchet distance.

for each $t \in [0, 1]$, $F(., t)$ is a homeomorphism onto its image.

An ambient isotopy between S and S' is a continuous map $F : \mathbb{R}^n \times [0, 1] \rightarrow \mathbb{R}^n$ such that $F(., 0)$ is the identity of \mathbb{R}^n , $F(S, 1) = S'$, and for each $t \in [0, 1]$, $F(., t)$ is a homeomorphism of \mathbb{R}^n . If the map F is C^k -smooth, it is called a C^k -smooth (ambient) isotopy.

Restricting an ambient isotopy between S and S' to $S \times [0, 1]$ thus yields an isotopy between them. If there exists an isotopy between S and S' , then there is an ambient isotopy between them [11], so that both notions are equivalent in our case.

1.2.4 Moat and median

Given two $(n-1)$ -manifolds S and S' , we define their moat and median (see figure 1.4). The *moat* of S and S' , $\text{Moat}(S, S')$ is:

$$\text{Moat}(S, S') = S \cup S' \cup (S_i \cap S'_e) \cup (S'_i \cap S_e)$$

or, equivalently:

$$\text{Moat}(S, S') = (S \cup S' \cup S_i \cup S'_i) \setminus (S_i \cap S'_i)$$

The *median* of S and S' , $\text{Me}(S, S')$ is defined as the set of points in $\text{Moat}(S, S')$ which are equidistant from S and S' :

$$\text{Me}(S, S') = \{x \in \text{Moat}(S, S') \mid d(x, S) = d(x, S')\}$$

Both $\text{Moat}(S, S')$ and $\text{Me}(S, S')$ are clearly compact sets. Notice that $S \cap S' \subset \text{Me}(S, S')$. Alternatively, the median can be defined as the locus of centers of closed balls included in the moat that intersect both S and S' .

1.3 Ball-compatibility and ball-map

We define now the main object of the paper: the ball-map.

Definition 1.3.1 (Ball-pair) Given two compact connected $(n-1)$ -manifolds S and S' in \mathbb{R}^n , we say that $(x, x') \in S \times S'$ is a ball-pair if there is $c \in \text{Me}(S, S')$ such that $d(c, x) = d(c, S) = d(c, x') = d(c, S')$.

Obviously, one has the following alternate definition.

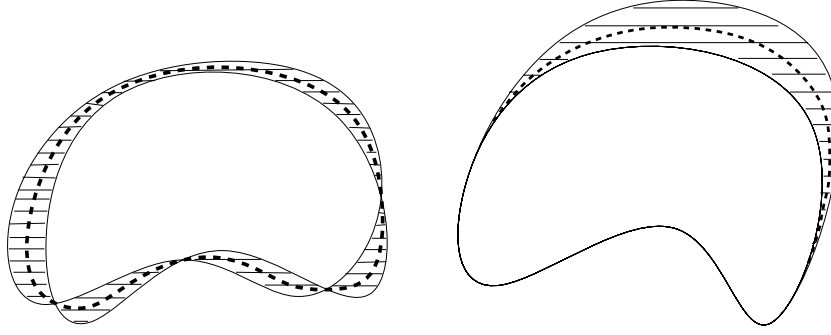


Figure 1.4: On both examples the moat is depicted as a hatched area and the median curve as a dashed line. In the example on the right, the curves S and S' overlap partially.

Definition 1.3.2 (Ball-pair, alternate definition) $(x, x') \in S \times S'$ is a ball-pair if and only if there is a closed ball $\mathbb{B} \subset \text{Moat}(S, S')$ such that $x \in \mathbb{B} \cap S$ and $x' \in \mathbb{B} \cap S'$.

It follows from this last definition that the ball-pairing is a conformal invariant, which means that any isometry or any inversion preserving the inner and outer connected components of $R^n \setminus S$ and $R^n \setminus S'$ will preserve the ball pairing.

If each point of S and each point of S' belongs to exactly one ball-pair, the ball pairing defines a bijection, which is then called the *ball-map*:

Definition 1.3.3 (Ball-compatibility) If each point of S and each point of S' belongs to exactly one ball pair, S and S' are said to be ball-compatible

Definition 1.3.4 (Ball-map) If S and S' are ball-compatible, the bijection $\text{BM}_{S,S'}$ and its inverse $\text{BM}_{S',S}$ defined by the ball pairing are called ball-maps.

Note that, when S and S' are ball compatible, the projections $\pi_S : \text{Me}(S, S') \rightarrow S$ and $\pi_{S'} : \text{Me}(S, S') \rightarrow S'$ that associates to each point of $\text{Me}(S, S')$ its unique closest point on S (resp. S') are also bijections and:

$$\text{BM}_{S,S'} = \pi_{S'} \circ \pi_S^{-1} \quad (1.2)$$

$$\text{BM}_{S',S} = \pi_S \circ \pi_{S'}^{-1} \quad (1.3)$$

When the manifolds are ball-compatible, the ball-map is a homeomorphism:

Lemma 1.3.5 If S and S' are ball-compatible, $\text{BM}_{S,S'}$ is a homeomorphism.

Proof. – It is clear that $\text{BM}_{S,S'}$, π_S and $\pi_{S'}$ are bijections. Recall that a continuous bijection between compact sets is a homeomorphism [7]. From equation (1.2), it is then enough to prove that $\pi_S : \text{Me}(S, S') \rightarrow S$ is continuous. For that, we consider, in the condition of the Lemma, a sequence of points $(c_n)_{n \in \mathbb{N}}$ in $\text{Me}(S, S')$ that converges to some $c \in \text{Me}(S, S')$. Let us denote by $(a_n)_{n \in \mathbb{N}}$ the respective closest points on S : $a_n = \pi_S(c_n)$. Because S is compact, there is at least one point a such that a subsequence $(a_{n_i})_{i \in \mathbb{N}}$ of $(a_n)_{n \in \mathbb{N}}$ converges toward a . S and S' being metric spaces, it is enough to prove that $a = \pi_S(c)$ to ensure the continuity of the map π_S . Because both the distance function and the distance to S are continuous, the sequence of distances $d(c_n, S)$ converges toward $d(c, S) = d(c, a)$, which entails that $a = \pi_S(c)$. \square

Note that Lemma 1.3.5 does not require any smoothness condition on the surfaces S and S' . It follows immediately from Lemma 1.3.5 and from its proof that:

Corollary 1.3.6 *If S and S' are ball-compatible, the median $\text{Me}(S, S')$ is a compact, connected $(n - 1)$ -manifold.*

Chapter 2

ball-compatibility

2.1 Conditions for ball-compatibility

2.1.1 Necessary and sufficient condition for C^1 manifolds

If we restrict ourselves to C^1 manifolds, one has the following necessary and sufficient condition for ball-compatibility:

Theorem 2.1.1 *Let S and S' be compact, connected C^1 $(n-1)$ -manifolds. S and S' are ball compatible if and only if the following conditions hold:*

- (i) $S_i \cap S'_i \neq \emptyset$
- (ii) $\text{Me}(S, S') \cap C(S) = \text{Me}(S, S') \cap C(S') = \emptyset$

Note that, as seen on figure 2.1, the theorem does not hold if we drop the C^1 condition.

Proof. – [Proof of Theorem 2.1.1]

The proof of the “only if” part of theorem 2.1.1 is rather trivial: indeed, if condition (ii) of the theorem does not hold, for example if $\text{Me}(S, S') \cap C(S) \neq \emptyset$, a point $c \in \text{Me}(S, S') \cap C(S)$ will have several closest point on S and the surfaces can not be ball-compatible. If the condition (i) does not hold, one has $\text{Moat}(S, S') = S \cup S' \cup S_i \cup S'_i$ and therefore $\text{Me}(S, S') = S \cap S'$. Since $S \neq S'$, there exists $x \in S \cup S' \setminus S \cap S'$ which cannot be in a ball-pair.

For the “if” part we prove first, using the C^1 smoothness and the condition (ii), that a point $x \in S$ cannot belong to more than one ball-pair:

Lemma 2.1.2 *If S and S' are compact, connected C^1 $(n-1)$ -manifolds such that $\text{Me}(S, S') \cap C(S') = \emptyset$ then any point $x \in S$ belongs to at most one ball-pair.*

Symmetrically, if $\text{Me}(S, S') \cap C(S) = \emptyset$, then any point $x \in S'$ belongs to at most one ball pair.

Proof. – Under the conditions of the Lemma, let us consider $x \in S$. If $x \in S \cap S'$, x belongs only to the zero radius ball corresponding to the unique ball-pair (x, x) . Now if for example $x \in S'_i$ (see figure 2.2), let us assume that it belongs to a ball-pair corresponding to a ball centered in c . Because $x \notin S'$ the ball has positive radius and, because S is C^1 , c must lie on the line through x orthogonal to the plane tangent to S

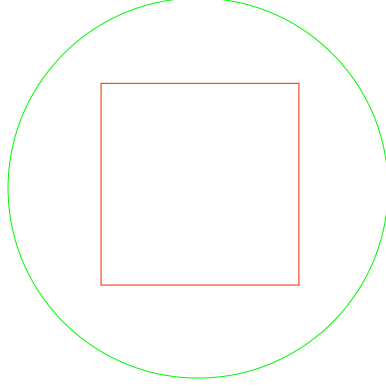


Figure 2.1: The square and circle curves are not ball-compatible (the square corners belong to many ball-pairs) even though they match all conditions of theorem 2.1.1, except the C^1 condition: the square is not smooth.

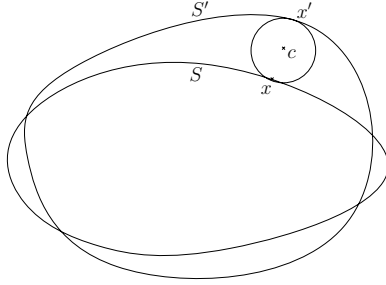


Figure 2.2: A point $x \in S \cap S'_i$ and its “ball-companion” $x' \in S'$.

at x . Moreover, because the ball is included in the moat, its radius $[c, x]$ is in the moat and then in $\overline{S_e}$. But there may be only one ball through x centered on the same half line orthogonal to the plane tangent to S at x and maximal in the moat. Therefore, the ball is unique and the condition of the Lemma implies that its center $c \in \text{Me}(S, S')$ is not in $C(S')$ so that there is only one $x' \in S'$ closest to c and x belongs to no other ball-pair. The case $x \in S'_e$ is similar. \square

We still have to prove that a point $x \in S$ belongs to at least one ball pair. For that, the main argument makes use of the fact that S_i and therefore (see [16]) $C_i(S)$ are connected and, for the outer part, that S_e is connected and unbounded, and therefore the connected components of $C_e(S)$, if any, are not bounded. This, together with condition (i) and (ii) of the theorem, shows that the median separates $C_i(S)$ and $C_e(S)$ (corollary 2.1.4). For that we consider the function $\psi : \mathbb{R}^n \rightarrow \mathbb{R}$:

$$\psi(x) = d\left(x, \overline{S_i} \cap \overline{S'_i}\right) - d\left(x, \overline{S_e} \cap \overline{S'_e}\right)$$

We let the reader check that:

$$\psi(x) = 0 \quad \Longleftrightarrow \quad x \in \text{Me}(S, S') \quad (2.1)$$

Hence, we may now introduce the open sets Me_i and Me_e :

$$\begin{aligned}\text{Me}_i(S, S') &= \{x \mid \psi(x) < 0\} \\ \text{Me}_e(S, S') &= \{x \mid \psi(x) > 0\}\end{aligned}$$

We have the following Lemma.

Lemma 2.1.3 *If condition (i) of theorem 2.1.1 holds, then:*

$$\begin{aligned}\text{Me}_i(S, S') \cap C_i(S) &\neq \emptyset \\ \text{Me}_i(S, S') \cap C_i(S') &\neq \emptyset\end{aligned}$$

In other words, a non-empty subset of the cut of S (and the cut of S') lies inside $\text{Me}_i(S, S')$.

Proof. — We prove here that $\text{Me}_i(S, S') \cap C_i(S) \neq \emptyset$.

Let us take $x \in S_i \cap S'_i$. Because $S_i \cap S'_i \subset \text{Me}_i(S, S')$, if $x \in C_i(S)$ one has $x \in \text{Me}_i(S, S') \cap C_i(S)$ and $\text{Me}_i(S, S') \cap C_i(S) \neq \emptyset$. Let us suppose now that $x \notin C_i(S)$. There is a unique $y \in S$ which is closest to x : $d(x, y) = d(x, S)$ and $y \neq x$. The half line $[yx$ cuts the closure of the medial axis $\overline{C_i(S)}$ at a point $x_0 \in \overline{C_i(S)}$. To see this, grows a ball centered at x and touching S at y by sliding its center on $[yx$ as long as it does not contain any other point of S and the boundary point of the set of such centers is x_0 . Recall that $x \in S_i \cap S'_i$. One has

$$d(x_0, \overline{S_e} \cap \overline{S'_e}) \geq d(x_0, \overline{S_e}) = d(x_0, y) > d(x_0, x) \geq d(x_0, \overline{S_i} \cap \overline{S'_i})$$

$x_0 \in \text{Me}_i(S, S')$ and $x_0 \in \overline{C_i(S)}$. But $\text{Me}_i(S, S')$ is open and this entails

$$\text{Me}_i(S, S') \cap C_i(S) \neq \emptyset$$

□

Lemma 2.1.3, implies the following.

Corollary 2.1.4 *If conditions (i) and (ii) of theorem 2.1.1 hold, then:*

$$\begin{aligned}C_i(S) &\subset \text{Me}_i(S, S') \\ C_e(S) &\subset \text{Me}_e(S, S') \\ C_i(S') &\subset \text{Me}_i(S, S') \\ C_e(S') &\subset \text{Me}_e(S, S')\end{aligned}$$

Proof. — Because S_i is connected, $C_i(S)$ is connected (see [16]). $\text{Me}(S, S') \cap C_i(S) = \emptyset$ (condition (ii) of the theorem) and equation (2.1) entails that ψ does not vanish on $C_i(S)$. Lemma 2.1.3 says us that ψ takes negative values on $C_i(S)$. Since ψ is continuous and $C_i(S)$ is connected, ψ is negative on $C_i(S)$. Similarly, because S_e is connected, the connected components of $C_e(S)$, if there are any, are unbounded and necessarily lies in $\text{Me}_e(S, S')$ (see Lemma 4.1.2). Again $\text{Me}(S, S') \cap C_e(S) = \emptyset$ allows us to conclude that $C_e(S) \subset \text{Me}_e(S, S')$. The two other properties follow from similar proofs. □

So we prove now that $x \in S$ is the closest point of some point $c \in \text{Me}(S, S')$. There are three possibilities for $x \in S$:

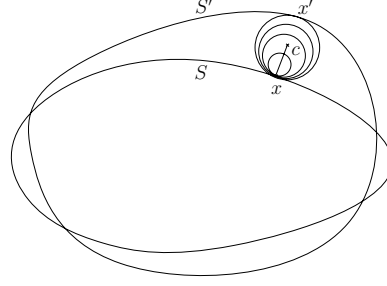


Figure 2.3: One can grow a small sphere contained in $\overline{S_e}$, tangent to S at x until its center coincides with c .

- (1) $x \in \text{Me}(S, S')$
- (2) $x \in \text{Me}_i(S, S')$
- (3) $x \in \text{Me}_e(S, S')$

In case (1), $x \in \text{Me}(S, S')$ and, trivially, x is the closest point to $c = x$.

In case (2), $x \in S$ and $x \in \text{Me}_i(S, S')$ entails $x \in S'_i$. The half-line starting at x and going outward S in the direction orthogonal to the plane tangent to S at x will cut the closed set $\text{Me}(S, S')$ at a first point $c \in \text{Me}(S, S')$. From Corollary 2.1.4, we have $C_e(S) \subseteq \text{Me}_e(S, S')$ and therefore $\text{Me}_i(S, S') \cap C_e(S) = \emptyset$ and, the segment $[x, c]$ being in $\text{Me}_i(S, S')$ cannot meet the outer medial axis $C_e(S)$. $x \in \text{Me}_i(S, S')$ entails that $d(x, C_e(S)) > 0$. Therefore, one can grow a small sphere (see figure 2.3) contained in $\overline{S_e}$, tangent to S at x until its center coincides with c . Consequently, x is the unique point of S closest to c . Case (3) is similar to case (2), using this time the relation $C_i(S) \subset \text{Me}_i(S, S')$ of Corollary 2.1.4. \square

2.1.2 A sufficient condition relying on Hausdorff distance

Given two surfaces S and S' sufficiently *close to each other* with respect to their minimum feature size, the *ball-map* is an homeomorphism between S and S' . More precisely:

Theorem 2.1.5 *Let S and S' be connected, compact $(n-1)$ -manifolds in R^n . If there exists $\varepsilon > 0$ such that $\text{mfs}(S) > \varepsilon$, $\text{mfs}(S') > \varepsilon$, and $d_H(S, S') < \varepsilon$, then the ball-pairing $\text{BM}_{S, S'}$ defines a homeomorphism between S and S' .*

We use the term *feature-respecting compatibility* to describe the condition of theorem 2.1.5. We show below that under the condition of this theorem, S and S' meet the conditions of theorem 2.1.1.

Proof. — We have seen in section 1.2.2 that $\text{mfs}(S) > \varepsilon$ (and $\text{mfs}(S') > \varepsilon$) entails that S (and S') are C^1 smooth.

One denotes by $S_e \downarrow^\varepsilon$ the erosion of S_e : this is the set of points in S_e whose distance to S is greater than ε . Similarly, one denotes by $S_i \downarrow^\varepsilon$ the set of points in S_i whose distance to S is greater than ε .

$$\begin{aligned} S_e \downarrow^\varepsilon &= \{x \in S_e : d(x, S) > \varepsilon\} \\ S_i \downarrow^\varepsilon &= \{x \in S_i : d(x, S) > \varepsilon\} \end{aligned}$$

$S'_e \downarrow^\varepsilon$ and $S'_i \downarrow^\varepsilon$ are defined accordingly.

We have the following lemma:

Lemma 2.1.6 *Let S and S' be connected, compact $(n-1)$ -manifolds in \mathbb{R}^n . If there exists $\varepsilon > 0$ such that $\text{mfs}(S) > \varepsilon$, $\text{mfs}(S') > \varepsilon$, and $d_H(S, S') < \varepsilon$ then*

$$\begin{aligned} S_i \downarrow^\varepsilon &\subset S'_i \quad \text{and} \quad S_e \downarrow^\varepsilon \subset S'_e \\ S'_i \downarrow^\varepsilon &\subset S_i \quad \text{and} \quad S'_e \downarrow^\varepsilon \subset S_e \end{aligned}$$

Notice that the condition $\text{mfs}(S) > \varepsilon$, $\text{mfs}(S') > \varepsilon$ is crucial. Indeed in the example of figure 1.3 one has $d_H(S, S') < \varepsilon$ for some small ε while the inclusions of the lemma does not hold.

Proof. – proof of Lemma 2.1.6

$d_H(S, S') < \varepsilon$ entails:

$$S_i \downarrow^\varepsilon \cup S_e \downarrow^\varepsilon \subset S'_i \cup S'_e$$

Because both $S_i \downarrow^\varepsilon$ and $S_e \downarrow^\varepsilon$ are connected (see [4]), they are each either a subset of the connected component S'_i or a subset of the connected component S'_e . Because $S_e \downarrow^\varepsilon$ is not bounded, it has to be a subset of S'_e . That is:

$$S_e \downarrow^\varepsilon \subset S'_e$$

Assume now that $S_i \downarrow^\varepsilon \subset S'_e$. Consequently

$$S_i \downarrow^\varepsilon \cup S_e \downarrow^\varepsilon \subset S'_e \quad (2.2)$$

We denote by $S^{+\varepsilon}$ the set of points at distance less than ε from S :

$$S^{+\varepsilon} = \{x \in \mathbb{R}^n : d(x, S) < \varepsilon\}$$

By taking the complement and then the interior of both terms of inclusion (2.2), we obtain

$$S'_i \subset S^{+\varepsilon} \quad (2.3)$$

We know (using a homotopy argument) that the medial axis $C_i(S')$ of S'_i is not empty [16]. Let us take $x' \in C_i(S')$. Because $\text{mfs}(S') > \varepsilon$, let us take $\alpha > 0$ such that $\varepsilon + \alpha < \text{mfs}(S')$.

The ball $\mathbf{B}_{x', \varepsilon + \alpha}$ centered at x' with radius $\varepsilon + \alpha$ is contained in S'_i :

$$\mathbf{B}_{x', \varepsilon + \alpha} \subset S'_i$$

And, from the inclusion (2.3):

$$\mathbf{B}_{x', \varepsilon + \alpha} \subset S^{+\varepsilon} \quad (2.4)$$

Because $\text{mfs}(S) > \varepsilon$, one has $x' \notin C(S)$. Let x be the unique point on S closest to x' . The line segment γ of length 2ε , centered at x supported by the line normal to S at x is included in $S^{+\varepsilon}$. Moreover, from $\text{mfs}(S) > \varepsilon$, the two boundary points of this line segment belong to the boundary of $S^{+\varepsilon}$. Note that $x' \in \gamma$. This is in contradiction with the inclusion (2.4). Consequently, the assumption $S_i \downarrow^\varepsilon \subset S'_e$ cannot happen. Hence, because $S_i \downarrow^\varepsilon$ is connected, we have $S_i \downarrow^\varepsilon \subset S'_i$. \square

An immediate consequence of lemma 2.1.6 is the following

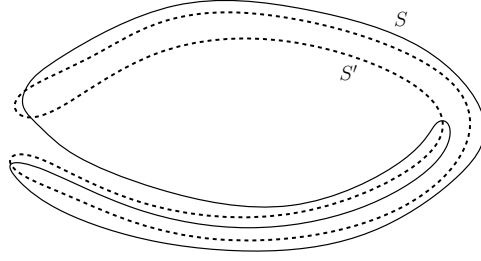


Figure 2.4: The two curves S and S' are ball compatible. Still $d_F(S, S') \neq d_H(S, S')$.

Corollary 2.1.7 *Let S and S' be connected, compact $(n-1)$ -manifolds in R^n with $\varepsilon > 0$ such that $\text{mfs}(S) > \varepsilon$, $\text{mfs}(S') > \varepsilon$, and $d_H(S, S') < \varepsilon$. Then:*

$$\begin{aligned} C_i(S) &\subset S'_i \quad \text{and} \quad C_e(S) \subset S'_e \\ C_i(S') &\subset S_i \quad \text{and} \quad C_e(S') \subset S_e \end{aligned}$$

In other words, S separates $C_i(S')$ from $C_e(S')$ and, symmetrically, S' separates $C_i(S)$ from $C_e(S)$.

Corollary 2.1.7 implies that, if $\text{mfs}(S) > \varepsilon$, $\text{mfs}(S') > \varepsilon$ and $d_H(S, S') < \varepsilon$, then one has $C_i(S) \subset S_i \cap S'_i$ and $C_e(S) \subset S_e \cap S'_e$. Therefore $\text{Me}(S, S') \cap C(S) = \emptyset$. One shows similarly that $\text{Me}(S, S') \cap C(S') = \emptyset$ and hence theorem 2.1.1 applies. \square

2.2 Bounding Fréchet distance

From the definition of the Fréchet distance (definition 1.2.2), taking an infimum on the set of homeomorphisms, we conclude that its computation for arbitrary (homeomorphic) pair of surfaces is expensive. In contrast, the definition of the Hausdorff distance whose nature is more geometric, makes it affordable.

We sketch a rough analysis of the complexity of computing Hausdorff distance. One can check that a compact, curvature bounded $(d-1)$ -manifold in R^d can be approximated up to ε in Hausdorff distance by a piecewise linear manifold of complexity (that is number of simplices) $n = O\left(\varepsilon^{-\frac{d-1}{2}}\right)$. We assume that the complexity of computing this approximation is no more than $O(n \log(n))$ which is reasonable for usual representations. On the other hand, the Hausdorff distance between two piecewise linear manifolds of complexity n can be computed (using spatial localization structure) in time $O(n \log(n))$. We obtain therefore an acceptable upper bound on the time complexity for computing an ε -approximation of the Hausdorff distance:

$$O\left(\varepsilon^{-\frac{d-1}{2}} \log\left(\frac{1}{\varepsilon}\right)\right)$$

Under the condition of ball-compatibility d_H can be arbitrary small with d_F arbitrarily large as suggested by figure 2.4.

However, we can show that, in the conditions of theorem 2.1.5, the Hausdorff and Fréchet distances are equal.

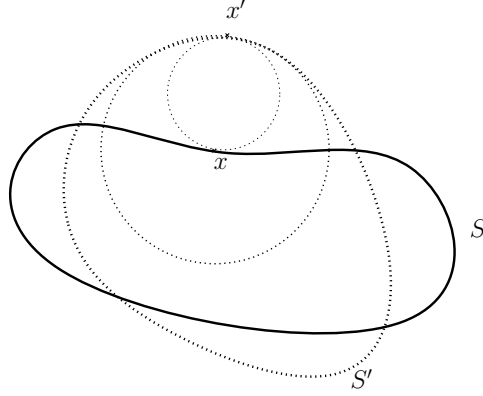


Figure 2.5: The ball centered at x and tangent to S' at x' contains no point of S' other than x' .

Theorem 2.2.1 *Let S and S' be connected, compact $(n-1)$ -manifolds in R^n with $\varepsilon > 0$ such that $\text{mfs}(S) > \varepsilon$, $\text{mfs}(S') > \varepsilon$, and $d_H(S, S') < \varepsilon$. Then:*

$$d_F(S, S') = d_H(S, S')$$

Proof. — The inequality $d_H(S, S') \leq d_F(S, S')$ holds in general and follows from the definitions of d_H and d_F . Because S is compact, there is a ball-pair $(x, x') \in S \times S'$, such that:

$$d(x, x') = \sup_{y \in S} d(y, \text{BM}_{S, S'}(y)) \geq d_F(S, S')$$

As seen in section 1.2.2 under the hypothesis of the theorem, both S and S' are C^1 . Therefore, in order for the distance $d(x, x')$ to be maximal among ball-pairs, the segment $[x, x']$ must be orthogonal to S at x and to S' at x' .

On the other hand, it follows from Lemma 2.1.6 that $\text{Moat}(S, S') \subset S'^\varepsilon$. But the segment $[x, x']$ being in $\text{Moat}(S, S') \subset S'^\varepsilon$ and orthogonal to S' at x' , it follows that $d(x, x') < \varepsilon$. But, because $\text{mfs}(S') > \varepsilon$, the ball of radius ε tangent to S' at x' , passing through x contains no point of S' other than x' . But this ball (see figure 2.5) contains the ball centered at x with radius $d(x, x')$: this implies that x' is the closest point to x on S' : $d(x, S') = d(x, x')$, and then:

$$d_F(S, S') \leq d(x, x') = d(x, S') \leq d_H(S, S')$$

□

Chapter 3

Properties of the Ball map

3.1 Smoothness

3.1.1 The smoothness of the ball-map

In the condition of theorem 2.1.5, the smoothness of $\text{BM}_{S,S'}$ is related to the smoothness of S and S' :

Theorem 3.1.1 (2.1.5 improved with smoothness of $\text{BM}_{S,S'}$) *In the conditions of theorem 2.1.5, $\text{BM}_{S,S'}$ is in fact Lipschitz and, if S and S' are C^k manifolds, with $k \geq 2$, then $\text{BM}_{S,S'}$ is a C^{k-1} diffeomorphism.*

Recall that we denote by $S^{+\varepsilon}$ the set of points at distance less than ε from S :

$$S^{+\varepsilon} = \{x \in \mathbb{R}^n : d(x, S) < \varepsilon\}$$

We start with a corollary of lemma 2.1.6. If one compares the definition of the moat with lemma 2.1.6, one gets:

Corollary 3.1.2 *Let S and S' be connected, compact $(n-1)$ -manifolds in \mathbb{R}^n with $\varepsilon > 0$ such that $\text{mfs}(S) > \varepsilon$, $\text{mfs}(S') > \varepsilon$, and $d_H(S, S') < \varepsilon$. Then:*

$$\begin{aligned} \text{Moat}(S, S') &\subset S^{+\varepsilon} \\ \text{Moat}(S, S') &\subset (S')^{+\varepsilon} \end{aligned}$$

Corollary 3.1.2 helps in the proof below.

Proof. –[proof of theorem 3.1.1]

When the surfaces are not C^2 and $\text{mfs}(S) > \varepsilon$, $\text{mfs}(S') > \varepsilon$, equation (1.1) in section 1.2.2 entails that \vec{n}_S and $\vec{n}_{S'}$ are $\frac{1}{\varepsilon}$ -Lipchitz. If moreover S is a C^k manifold with $k \geq 2$ $x \mapsto \vec{n}_S(x)$ is a C^{k-1} map.

Let us consider the map $\varphi : S \times \mathbb{R} \rightarrow \mathbb{R}^n$ defined by:

$$\varphi(x, t) = x + t \cdot \vec{n}_S(x)$$

$\varphi' : S' \times \mathbb{R} \rightarrow \mathbb{R}^n$ is defined similarly. Notice that if $x' = \text{BM}_{S,S'}(x)$, then, there exists $t \in (-\varepsilon, \varepsilon)$ such that:

$$\varphi(x, t) = \varphi'(x', -t)$$

Indeed, if $x \in S \cap S'$, the equality holds for $t = 0$.

If $x \in S \setminus S \cap S'$, then either the ball map is defined by a ball in $\overline{S_i \cap S'_e}$, in which case its center y satisfies $y = \varphi(x, t)$ for some $t < 0$, or the ball-map is defined through a ball in $\overline{S_e \cap S'_i}$, in which case its center y satisfies $y = \varphi(x, t)$ for some $t > 0$.

Define the map $F : S \times S' \times \mathbb{R} \rightarrow \mathbb{R}^n$ as

$$F(x, x', t) = \varphi(x, t) - \varphi'(x', -t)$$

Locally, the implicit equation $F(x, x', t) = 0$ defines the ball-map:

$$x' = \text{BM}_{S, S'}(x) \Rightarrow \exists t : F(x, x', t) = 0 \text{ and } \varphi(x, t) \in \text{Moat}(S, S')$$

We check below that the implicit functions theorem applies and it follows that the relation $F(x, x', t) = 0$ defines locally a C^{k-1} smooth one-to-one mapping: $x \mapsto (x'(x), t(x))$ such that $F(x, x'(x), t(x)) = 0$. In order to express the derivative of the map φ' at $x' \in S'$ by a matrix, one chooses a convenient local coordinate system for S' and \mathbb{R}^n . It is a classic result that, when $\text{mfs}(S) > \varepsilon$, $\varphi : S \times (-\varepsilon, \varepsilon) \rightarrow S^{+\varepsilon}$ is one-to-one, but we give the proof here for completeness.

Let us take an orthonormal frame centered at x' , with last vector being the unit normal to S' at $x' \in S'$ pointing outward. This defines a frame in \mathbb{R}^n . Notice that, with the origin x' , the first $n-1$ vectors of the frame define an orthogonal frame for the plane tangent to S' at x' .

The orthogonal projection of S' on its tangent plane at x' defines a local coordinate system for S' , using the same $(n-1)$ orthonormal frame of the tangent plane defined above. Using these maps for S' and \mathbb{R}^n , it is possible to write the derivative of φ' with respect to x' and t in the form of a matrix. In the expression below, the first column and row correspond to the $n-1$ tangential directions and the second column and row to the normal direction to S' at x' . One denotes by $\mathbf{1}$ the $(n-1) \times (n-1)$ unit matrix. One has

$$\begin{pmatrix} \frac{\partial \varphi'}{\partial x'} & \frac{\partial \varphi'}{\partial t} \end{pmatrix} = \begin{pmatrix} \mathbf{1} + t \cdot \frac{\partial \overrightarrow{n_{S'}}(x')}{\partial x'} & 0 \\ 0 & 1 \end{pmatrix}$$

Notice that, with the chosen maps, $\frac{\partial \overrightarrow{n_{S'}}(x')}{\partial x'}$ is precisely the derivative of the Gauss map of S' at x' . If $F(x, x', t) = 0$, one has either $t = 0$ or $\varphi'(x', t) \in \text{Moat}(S, S')$. Thus, from corollary 3.1.2, one has $t < \varepsilon$. Using equation (1.1), we obtain:

$$\left\| t \cdot \frac{\partial \overrightarrow{n_{S'}}(x')}{\partial x'} \right\| < 1 \quad (3.1)$$

It follows that the $(n-1) \times (n-1)$ determinant $|\mathbf{1} + t \cdot \frac{\partial \overrightarrow{n_{S'}}(x')}{\partial x'}|$ does not vanish:

$$\left| \mathbf{1} + t \cdot \frac{\partial \overrightarrow{n_{S'}}(x')}{\partial x'} \right| \neq 0$$

Consequently:

$$\begin{pmatrix} \frac{\partial F}{\partial x'} & \frac{\partial F}{\partial t} \end{pmatrix}$$

has a non-zero determinant and therefore full rank, which allows to apply the implicit function theorem: there are C^{k-1} maps $x \mapsto x'(x)$ and $x \mapsto t(x)$ defined in a neighborhood of x such that $F(x, x'(x), t(x)) = 0$. Therefore, $\text{BM}_{S, S'}$ and $\text{BM}_{S, S'}$ are C^{k-1} , which proves the theorem when the surfaces are at least C^2 .

When the surfaces are not C^2 , but only with positive mfs, one cannot apply the usual implicit function theorem. The local inversion can be built explicitly: using a weak

version of equation (3.1), it is possible to inverse the map φ' explicitly, as the fix point of an iterative inversion algorithm. Alternatively, one can use a Lipschitz variant of the implicit function theorem (see Clarke [5]). \square

3.1.2 Smoothness of the median surface

As stated in theorem 3.1.1, the map $\text{BM}_{S,S'}$ loses one order of continuity with respect to S and S' : if S and S' are C^k , then the ball-map is C^{k-1} only. This behavior is not a surprise if we recall the central role of the Gauss maps \vec{n} and \vec{n}' , which are of course C^{k-1} . Consequently, $\text{Me}(S, S')$ is then a C^{k-1} manifold. We prove that $\text{Me}(S, S')$ is in fact not only C^{k-1} but C^k .

Theorem 3.1.3 *Let S and S' be connected, compact $(n-1)$ -manifolds in R^n with $\varepsilon > 0$ such that $\text{mfs}(S) > \varepsilon$, $\text{mfs}(S') > \varepsilon$, and $d_H(S, S') < \varepsilon$. Then, the Gauss map $\vec{n}_{\text{Me}(S, S')}$ of the median surface $\text{Me}(S, S')$ is ε -Lipschitz. Moreover, if S and S' are C^k manifolds, then $\text{Me}(S, S')$ is a C^k manifold.*

The proof of the theorem is based upon the characterization of $\text{Me}(S, S')$ with distance functions to S and S' . For that, one uses the following Lemma.

Lemma 3.1.4 *Let S and S' be connected, compact $(n-1)$ -manifolds in R^n with $\varepsilon > 0$ such that $\text{mfs}(S) > \varepsilon$, $\text{mfs}(S') > \varepsilon$, and $d_H(S, S') < \varepsilon$. Let $x \in S$, $x' \in S'$ and $c \in \text{Me}(S, S')$ be such that x (resp. x') is the point of S (resp. S') closest to c . Let $\Pi_{x,S}$, $\Pi_{x',S'}$ and $\Pi_{c, \text{Me}(S, S')}$ be the respective tangent planes at x , x' and c on the respective surfaces S , S' and $\text{Me}(S, S')$.*

Then:

- (1) *if $x \neq x'$, $\Pi_{c, \text{Me}(S, S')}$ is the bisector of the points x and x'*
- (2) *$\Pi_{c, \text{Me}(S, S')}$ is the bisector of the planes $\Pi_{x,S}$ and $\Pi_{x',S'}$*

Proof. — The fact that, if $x \neq x'$, the bisector of the points x and x' happen to be the bisector of the planes $\Pi_{x,S}$ and $\Pi_{x',S'}$ results from the observation that the triangle xcx' is isosceles and that the planes $\Pi_{x,S}$ and $\Pi_{x',S'}$ are orthogonal respectively to cx and cx' . It is then enough to prove (2).

The distance function to S , $\mathbf{d}_S : \mathbb{R}^n \rightarrow \mathbb{R}^+$ is 1-Lipschitz and is differentiable at any point that does not belong to the closure of the cut \bar{C} . In particular, it is differentiable at $c \in \text{Moat}(S, S')$. Without loss of generality, assume that $c \in S_i \cap S'_e$. In this case, if one denotes by $\nabla \mathbf{d}_S$ the gradient of \mathbf{d}_S , one has:

$$\nabla \mathbf{d}_S(c) = -\vec{n}(x)$$

and, similarly:

$$\nabla \mathbf{d}_{S'}(c) = \vec{n}'(x')$$

Therefore, the map $c \mapsto \mathbf{d}_{S'}(c) - \mathbf{d}_S(c)$ is differentiable and has gradient:

$$\nabla (\mathbf{d}_{S'} - \mathbf{d}_S)(c) = \vec{n}(x) + \vec{n}'(x')$$

We claim that this gradient cannot be 0:

$$\vec{n}(x) + \vec{n}'(x') \neq 0, \quad (3.2)$$

Indeed, if $x = x'$, the relation (3.2) holds (if not, there exists a $\lambda > 0$ such that $x + \lambda \vec{n}(x) \in \text{Moat}(S, S')$ which leads to a contradiction). Otherwise, if $x \neq x'$, one has $\|\vec{cx}\| = \|\vec{cx'}\| = t > 0$, $\vec{cx} = t \vec{n}(x)$, and $\vec{cx'} = -t \vec{n}'(x')$. Therefore:

$$\vec{n}(x) + \vec{n}'(x') = \frac{1}{t} \vec{cx}$$

Which proves (3.2).

Then, it follows from the implicit function theorem, that the surface $\text{Me}(S, S')$ has a tangent plane at c that is normal to the vector $\vec{n}(x) + \vec{n}'(x')$. \square

The previous Lemma allows us to prove the smoothness of C :

Proof. – Proof of Theorem 3.1.3

In the proof of Lemma 3.1.4 above, we show that the implicit function theorem applies to the map $c \mapsto \mathbf{d}_{S'}(c) - \mathbf{d}_S(c)$. If S and S' are C^k manifolds, this map is C^k and, by the implicit function theorem, $\text{Me}(S, S')$ is a C^k manifold. \square

3.2 Ball-map surface encoding

Let S and S' be C^1 ball-compatible surfaces. let $r(x)$ denotes the radius of the ball corresponding to the ball-pair $(x, \text{BM}_{S, S'}(x))$. The signed scalar field $\rho : S \rightarrow \mathbb{R}$ is defined by:

$$\rho(x) = \begin{cases} r(x) & \text{if } x \in S \cap S'_e, \\ 0 & \text{if } x \in S \cap S', \\ -r(x) & \text{if } x \in S \cap S'_i \end{cases}$$

If the surface S is known, it is possible to retrieve the surface S' from the scalar field ρ . We say that ρ encodes the surface S' .

Let us denote $\mathbb{B}_{(0,1)} \subset \mathbb{R}^n$ the unit ball in \mathbb{R}^n and by $\Phi : \mathbb{B}_{(0,1)} \times S \rightarrow \mathbb{R}^n$ the map defined by:

$$\Phi(v, x) = x + \rho(x)(\vec{n}_S(x) + v) \quad (3.3)$$

Any ball corresponding to a ball-pair is included in $\text{Moat}(S, S')$ and one can see that any point in the moat belongs to the ball corresponding to its closest point on S .

We have therefore:

$$\text{Moat}(S, S') = \bigcup_{x \in S} \Phi(\mathbb{B}_{(0,1)}, x) = \Phi(\mathbb{B}_{(0,1)}, S)$$

We are interested in the boundary of the moat: $\partial \text{Moat} = S \cup S'$. For that we look at the pairs $(v, x) \in \mathbb{B}_{(0,1)} \times S$. First notice that if $\rho(x) \neq 0$ and if v is in the interior $\mathbb{B}_{(0,1)}^\circ$ of $\mathbb{B}_{(0,1)}$ the couple (v, x) has its image in the interior of $\Phi(\mathbb{B}_{(0,1)}, x)$ because, if $B_v \subset \mathbb{B}_{(0,1)}$ is a small ball centered at v , $\Phi(B_v, x)$ is a small ball centered at $\Phi(v, x)$.

So we restrict now to pairs $(v, x) \in \mathbb{S}^{n-1} \times S$, where \mathbb{S}^{n-1} is the unit sphere in \mathbb{R}^n . We consider now a local map (that is a regular parameterization) in a neighborhood N_v of v on \mathbb{S}^{n-1} and a local map on a neighborhood N_x of x on S . We denote respectively by $U_x \subset \mathbb{R}^{n-1}$ and $U_v \subset \mathbb{S}^{n-1}$ the domains of the local maps. The maps are denoted

respectively $\mathbf{x} : U_x \rightarrow N_x$ and $\mathbf{v} : U_v \rightarrow N_v$ and the parameters respectively u and w so that one can write $x = \mathbf{x}(u)$ and $v = \mathbf{v}(w)$. Recall that in this section S and S' are assumed to be C^1 . Without loss of generality, the parameterization of S can be chosen in such a way that the $n-1$ partial derivatives $\frac{\partial \mathbf{x}}{\partial u^k}, k = 1, \dots, n-1$ makes an orthonormal basis of the plane tangent to S at x .

One denotes by $\hat{\Phi}$ the map Φ seen as a function of the parameter (w, u) :

$$\hat{\Phi}(w, u) = \Phi(\mathbf{v}(w), \mathbf{x}(u))$$

By a standard argument in differential geometry, if the derivatives $\frac{\partial \hat{\Phi}}{\partial u}, \frac{\partial \hat{\Phi}}{\partial w}$ (seen as a $n \times (2n-2)$ matrix) has rank n , that is if its columns span the n -dimensional space R^n , the image of (v, x) is necessary in the interior of $\Phi(\mathbb{B}_{(0,1)}, S)$. Therefore, for a couple (v, x) to have its image on the boundary, one must have:

$$\text{rank} \left(\frac{\partial \hat{\Phi}}{\partial u}, \frac{\partial \hat{\Phi}}{\partial w} \right) < n \quad (3.4)$$

But we know that $\frac{\partial \hat{\Phi}}{\partial w}$ span precisely the plane tangent to \mathbb{S}^{n-1} at v so that equation (3.4) implies that $\frac{\partial \hat{\Phi}}{\partial u}$ span the same hyperplane. In other words, for a couple (v, x) to have its image on the boundary, all the columns of $\frac{\partial \hat{\Phi}}{\partial u}$ must be orthogonal to v . We obtain from (3.3):

$$\frac{\partial \hat{\Phi}}{\partial u} = \frac{\partial \mathbf{x}}{\partial u} + \frac{\partial \rho}{\partial u} (\vec{n}_S(x) + v) + \rho(x) \frac{\partial \vec{n}_S(\mathbf{x})}{\partial u}$$

Note that, because the local system of coordinates $u \mapsto \mathbf{x}(u)$ is such that the vectors $\frac{\partial \mathbf{x}}{\partial u_k}(u)$, for $k = 1, \dots, n-1$ make a normalized orthogonal basis of the plane tangent at $x = \mathbf{x}(u)$, the coordinates of:

$$\frac{\partial \vec{n}_S(\mathbf{x})}{\partial u_i}$$

in the basis $\frac{\partial \mathbf{x}}{\partial u_k}(u)$, for $k = 1, \dots, n-1$ expresses the normal curvature of S at x .

Still without loss of generality, the coordinate system can be taken such that $\frac{\partial \mathbf{x}}{\partial u_1}$ is in the direction of the gradient of $x \mapsto \rho(x)$, that is: $\frac{\partial \rho(\mathbf{x}(u))}{\partial u_1} > 0$ and $\frac{\partial \rho(\mathbf{x}(u))}{\partial u_i} = 0$, for $i = 2, \dots, n-1$. Let us denote by \vec{U}_i the vector $\vec{U}_i = \frac{\partial \hat{\Phi}}{\partial u_i}$. For $i = 2, \dots, n-1$, one has:

$$\vec{U}_i = \frac{\partial \mathbf{x}}{\partial u_i} + \rho(x) \frac{\partial \vec{n}_S(\mathbf{x})}{\partial u_i}$$

and, for $i = 2, \dots, n-1$, \vec{U}_i is orthogonal to \vec{n}_S . In the conditions of ball-compatibility, the normal curvature of S at x is bounded by $\frac{1}{\rho(x)}$. If this curvature is strictly bounded

by $\frac{1}{\rho(x)}$ then the norm of $\rho(x) \frac{\partial \vec{n}_S(\mathbf{x})}{\partial u_i}$ is strictly bounded by 1 and for $i = 2, \dots, n-1$, \vec{U}_i span a $(n-2)$ -dimensional linear subspace of the plane tangent to S at x .

Let us denote by \vec{W} a unit vector in the plane tangent to S at x orthogonal to U_i for $i = 2, \dots, n-1$. Note that \vec{W} is uniquely determined up to a change of sign. Notice that the vectors \vec{W} and \vec{n}_S make a normalized, orthogonal basis of the plane orthogonal to $\vec{U}_2, \vec{U}_3, \dots, \vec{U}_{n-1}$. Our goal is to compute the vector v . Because v is orthogonal to

the \vec{U}_i , it belongs to the plane spanned by \vec{W} and \vec{n}_S . This, together with the relation $v \cdot \vec{U}_1 = 0$ allow to determine v .

One has:

$$\vec{U}_1 = \frac{\partial \mathbf{x}}{\partial u_1} + \frac{\partial \rho}{\partial u_1}(\vec{n}_S(x) + v) + \rho(x) \frac{\partial \vec{n}_S(\mathbf{x})}{\partial u_1}$$

One can write: $v = \lambda \vec{W} + \mu \vec{n}_S(x)$ where λ and μ can be determined by $\lambda^2 + \mu^2 = 1$ and $v \cdot \vec{U}_1 = 0$. If one rewrite \vec{U}_1 as $\vec{U}_1 = \vec{V}_1 + \frac{\partial \rho}{\partial u_1} v$, the second equation on λ and μ can be written:

$$\left(\lambda \vec{W} + \mu \vec{n}_S(x) \right) \cdot \left(\vec{V}_1 + \frac{\partial \rho}{\partial u_1} \left(\lambda \vec{W} + \mu \vec{n}_S(x) \right) \right) = 0$$

This leads to a degree 2 equation. Because $\vec{n}_S(x) \cdot \vec{V}_1 = \frac{\partial \rho}{\partial u_1}$, one trivial solution is $\lambda = 0$ and $\mu = -1$ which corresponds to $v = -\vec{n}_S(x)$ and $\Phi(v, x) = x \in S$. This “trivial” solution appears because S contributes also to the boundary of the moat. The other solution of the equation gives us the wanted vector v and finally $\Phi(v, x) = \text{BM}_{S, S'}(x) \in S'$.

3.3 Implementation

In this section, we outline two implementations for computing the image x' in S' of a point x in S by the ball-map $\text{BM}_{S, S'}$ assuming that S' and S are ball-compatible. A detailed and rigorous description of implementation is beyond the scope of the present paper.

3.3.1 Piecewise-circular curves

First, we consider the case where S and S' are piecewise-circular manifold curves (see [24] and [19]) in the plane, each composed of a finite number of smoothly joining segments. A segment j is either a straight-line segment or a circular arc of less than 180 degrees. Let $\text{ext}(j)$ be the extent of j , i.e. the line or circle that contain j . In this case, the ball-map can be computed efficiently and precisely. For each segment j of S' , we compute the signed distance d_j , such that $d_j = \text{dist}(x + d_j \vec{n}_S, \text{ext}(j))$, where \vec{n}_S is the unit normal to S at x oriented towards the moat (the orientation of \vec{n}_S is not defined in areas where the S and S' coincide, since there is no moat, but the ball pairs are coincident). When j is a line segment, assuming that $\text{ext}(j)$ is represented by a point z on it and by a normal \vec{n}_j , d_j may be obtained by solving:

$$(\vec{z}x + d_j \vec{n}_S) \cdot \vec{n}_j = d_j$$

which yields $d_j = \frac{\vec{z}x \cdot \vec{n}_j}{1 - \vec{n}_S \cdot \vec{n}_j}$

When j is a circular arc, assuming that $\text{ext}(j)$ is represented by its center z_j and radius r_j , d_j may be obtained by solving $(\vec{z}_j x + d_j \vec{n}_S)^2 = (d_j + r_j)^2$, which yields $(\vec{z}_j x + d_j \vec{n}_S) \cdot (\vec{z}_j x + d_j \vec{n}_S) = d_j^2 + 2r_j d_j + r_j^2$. Distributing the dot-product over vector addition and replacing $\vec{n}_S \cdot \vec{n}_S$ by 1, we obtain: $\vec{z}_j x^2 + 2(\vec{z}_j x \cdot d_j \vec{n}_S) + d_j^2 = d_j^2 + 2r_j d_j + r_j^2$, which yields

$$d_j = \frac{(\vec{z}_j x)^2 - r_j^2}{2r_j - 2\vec{z}_j x \cdot \vec{n}_S}$$

Note that the formulation proposed above may lead to a division by zero. To avoid those, the corresponding special cases are detected and processed explicitly. Furthermore, this formulation may lead to large round-off errors for arcs with extremely large radius. To avoid these, we represent each circular arc j by its two endpoints, A_j and B_j , and by the signed maximum deviation distance D_j between arc j and the straight-line segment joining A_j and B_j . Once d_j is obtained, we compute the closest projection y_j of $m = x + d_j \vec{n}_S$ onto $\text{ext}(j)$. Note that by construction $\|xm\| = \|y_j m\| = d_j$. Finally, from the set of candidate points y_j that are contained in their segment j , we select the one with the smallest positive d_j . It is the image x' of x by $\text{BM}_{S,S'}$.

3.3.2 Triangle-mesh approximations

Now, consider the delicate case where S and S' are defined as limits of sequences of triangle-meshes obtained through subdivision of a coarse mesh. To compute the image x' on S' of vertex x of S , we must compute d such that the distance from $x + d \vec{n}_S$ to S' is d where \vec{n}_S is the normal to S estimated at x . As we did in the 2D case, the image of x is the point x' closest to $x + d \vec{n}_S$ for the smallest value of d . The natural approach is to consider candidates x'_j for x' on the vertices, edges, and triangles of S' . When the candidate x'_j is a vertex of S' , d_j is computed as the solution of $(\vec{x'_j x} + d_j \vec{n}_S)^2 = d_j^2$, which yields

$$d_j = -\frac{(\vec{x'_j x})^2}{2\vec{x'_j x} \cdot \vec{n}_S}$$

When x'_j is assumed to lie on the plane through z_j , with normal \vec{n}_j , that contains a triangle of S' , d_j may be obtained by solving $(\vec{x'_j x} + d_j \vec{n}_S) \cdot \vec{n}_j = d_j$, which yields

$$d_j = \frac{\vec{x'_j x} \cdot \vec{n}_j}{1 - \vec{n}_S \cdot \vec{n}_j}$$

We must test whether x'_j lies within the triangle. Finally, when x'_j is assumed to lie on the line containing an edge of S' , we compute d_j as the smallest root of a quadratic equation. We discard points x'_j that do not lie on the edge. Note that this approach may produce more than one image, since different polygonal models are by definition not ball-compatible (their minimum feature size is zero and their Hausdorff distance is not). Selecting any one of these solutions on the triangle mesh produces acceptable approximations of the ball-map between the limit surfaces. Furthermore, the error may be diminished by increasing the level of subdivision.

Chapter 4

The conformal point of view

4.1 Ball-map and conformal invariance

4.1.1 Conformal group

Given a point $c \in \mathbb{R}^n$ and $r > 0$, the *inversion* I with respect to the sphere of center c and radius r is given by:

$$I(x) = c + \frac{r^2}{(x - c)^2} (x - c)$$

Notice that points on the sphere with center c and radius r are invariant by the action of I . Points inside the sphere are sent outside, while the points outside are sent inside. It is easier to work in the compact space $\mathbb{R}^n \cup \{\infty\}$. In this case I is extended as:

$$\begin{aligned} I(c) &= \infty \\ I(\infty) &= c \end{aligned}$$

Notice that with this complete definition, I is one-to-one from $\mathbb{R}^n \cup \{\infty\}$ to $\mathbb{R}^n \cup \{\infty\}$. It is even a homeomorphism if one considers the usual topology that makes $\mathbb{R}^n \cup \{\infty\}$ compact. The *conformal group* is the group of transformations obtained from the compositions of inversions and isometries. We call here *oriented sphere* any object in one of the following classes:

- closed balls of possibly 0 radius
- complement of open balls of possibly 0 radius which includes the whole space $\mathbb{R}^n \cup \{\infty\}$ itself
- closed linear half spaces

Even if they look more like balls, we call them oriented spheres because they are defined by a sphere and an orientation. Transformations of the conformal group transform planes and spheres into planes or spheres. Therefore we have the following proposition needed in the next section.

Proposition 4.1.1 *The image of an oriented sphere by a transformation of the conformal group is an oriented sphere.*

A smooth map $f : \mathbb{R}^n \rightarrow \mathbb{R}^n$ is said to be *conformal* if it preserves the angles “locally”. This means that, for any point $x \in \mathbb{R}^n$ the derivative $df(x)$, as linear transformation of \mathbb{R}^n , preserves angles and is therefore the product of a scaling and an isometry. For $n \geq 3$ the conformal maps $f : \mathbb{R}^n \rightarrow \mathbb{R}^n$ are precisely the transformations obtained by composition of scaling, isometries and inversions.

We are now equipped to prove a small lemma used in the proof of Lemma 2.1.4:

Lemma 4.1.2 *If S is a compact, connected $(n-1)$ -manifold embedded in \mathbb{R}^n , the connected components of $C_e(S)$, if there are any, are unbounded.*

Proof. — If, starting from S we apply an inversion I with respect to a center in the inner connected component of $\mathbb{R}^n \setminus S$, we obtain a compact, connected $(n-1)$ -manifold $\hat{S} = I(S)$. Notice that the inversion I exchanges the inner and outer components of the complement in $\mathbb{R}^n \cup \{\infty\}$. Then $C_i(\hat{S})$, the inner component of the cut of \hat{S} is connected (see [16]), and is homeomorphic to the set $\Sigma_i(\hat{S})$ of balls (or equivalently, oriented spheres) inside the bounded connected component of $\mathbb{R}^n \setminus \hat{S}$ and intersecting \hat{S} in at least two points. This connected set is homeomorphic to the set $\Sigma_e(S) = I(\Sigma_i(\hat{S}))$ of oriented spheres outside S , intersecting S in at least two points. If CC is a connected components of $C_e(S)$, it must be homeomorphic to some subsets $\sigma(CC)$ of the connected set $\Sigma_e(S)$. But $\Sigma_e(S)$ must contain at least one oriented sphere of type “complement of open ball” and it must therefore be a path in $\Sigma_e(S)$ connecting $\sigma(CC)$ and this oriented sphere, which is impossible if CC is bounded. \square

The definition of conformal maps extends to surfaces with metrics. A smooth map $f : S \rightarrow S'$ between two embedded or Riemann surfaces is said *conformal* if it preserves the angles “locally”: for any point $x \in S$ the derivative $df(x)$, as linear map from the tangent plane $T(x)$ at x to the tangent plane $T(f(x))$ at $f(x)$ preserves angles, and is therefore the product of a scaling and an isometry.

4.1.2 Generalizing ball-map

The definition of the ball-map relies on the definition of the middle-set, bisector of $\overline{S_i} \cap \overline{S'_i}$ and $\overline{S_e} \cap \overline{S'_e}$. The notion of bisector relies of course on the Euclidean metric. It follows that the ball-map is obviously invariant by isometry, which means that applying the same distance preserving transformation of the ambient space to two surfaces S and S' will trivially preserve their ball-pairing. The same invariance extends obviously for scaling transformations. We have seen (definition 1.3.2) that the definition of ball-pairing is invariant under inversions with both centers in $S_e \cap S'_e$. Indeed, under such an inversion, the images of maximal balls contained in the moat remains maximal balls contained in the moat which enforces the invariance of the pairing relation under such inversions.

Now, if one considers an inversion I with respect to a point in S_i , the inversion will turn S_i into an unbounded set $I(S_i)$ outside $I(S)$. We have therefore to amend our definition if we want a complete conformal invariance. This time we do not assume S nor S' to be bounded, but only to be codimension 1 connected and boundaryless and with only one point at the infinity (in other words, images of compact embedded $(n-1)$ -manifolds of \mathbb{S}^n by the stereographic projection $\text{Stereo} : \mathbb{S}^n \rightarrow \mathbb{R}^n \cup \{\infty\}$). They are given an orientation so that S separates \mathbb{R}^n into three connected components, S itself, S^- and S^+ . Similarly, S' separate \mathbb{R}^n into three connected components, S' itself, S'^- and S'^+ . S and S' can still be regarded as compact if one considers them as subset of the compact

space $R^n \cup \{\infty\}$. In this context, we define a *generalized moat*:

$$\text{Moat}^*(S, S') = (\overline{S^+} \cup \overline{S'^+}) \setminus (S^+ \cap S'^+)$$

Note that this time the surfaces bear an orientation and that the definition of the moat depends on this orientation and no more on orientation induced by the bounded/unbounded sides.

Definition 4.1.3 (Generalized ball-pairing) *The pair $(x, x') \in S \times S'$ is said to be a ball-pair if there is an oriented sphere σ such that:*

$$\begin{aligned} \sigma &\subset \text{Moat}^*(S, S') \\ \{x\} &= \sigma \cap S \\ \{x'\} &= \sigma \cap S' \end{aligned}$$

Definition 4.1.4 (Generalized ball-compatibility) *Two oriented surfaces S and S' are said to be compatible for the generalized ball-map if the generalized ball pairing is one-to-one.*

In this situation, x' is uniquely determined for a given x and one writes $\text{BM}_{S, S'}^*(x) = x'$. Conformal transformations map oriented spheres into oriented spheres and preserve the inclusion order. hence:

$$x' = \text{BM}_{S, S'}^*(x) \iff I(x') = \text{BM}_{I(S), I(S')}^*(I(x))$$

Therefore, when the center of the inversion I is neither on S nor S' , $\text{BM}_{S, S'}^*$ defines an homeomorphism if and only if $\text{BM}_{I(S), I(S')}^*$ defines a homeomorphism.

If the center of the inversion is on S or S' , the property remains true if one consider the compact space $R^n \cup \{\infty\}$. Therefore, we have:

Proposition 4.1.5 *The generalized ball-map is a conformal invariant.*

This generalization allows us to consider the ball-map in new situations. Indeed, consider S and S' bounded such that S^- and S'^+ are the bounded connected components and $S^- \cap S'^+ = \emptyset$: S and S' can not be ball compatible as the bounded connected components have empty intersection. However, according to the generalized definition they are compatible for the generalized ball-map. For example, figure 4.2 depicts the generalized ball-map between two disjoint spheres. Moreover, in this particular case, the generalized ball-map is itself conformal, which means that it locally preserves the angles.

Proposition 4.1.6 *The generalized ball-map between two spheres or between a sphere and a plane is conformal.*

Proof. — We first claim that the classical stereographic projection between a sphere of center $(0, \dots, 0, 1)$ and radius 1 with the plane $\{(x_1, \dots, x_n) : x_n = 0\}$ is the generalized ball-map between the sphere and the plane with the orientation defined such that S^- is the ball bounded by the sphere and S'^- is the half-space $\{(x_1, \dots, x_n) : x_n \geq 0\}$.

Indeed, consider the figure 4.3. The large circle is the sphere of center \mathbf{O} with coordinates $(0, \dots, 0, 1)$ and radius 1, and “north pole” \mathbf{N} , with coordinates $(0, \dots, 0, 2)$, while the small sphere is the oriented sphere with center \mathbf{O}' touching the plane at the

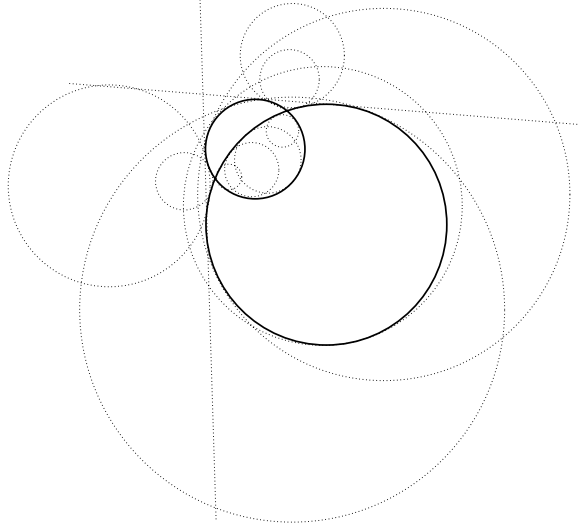


Figure 4.1: Generalized ball-map between two intersecting spheres

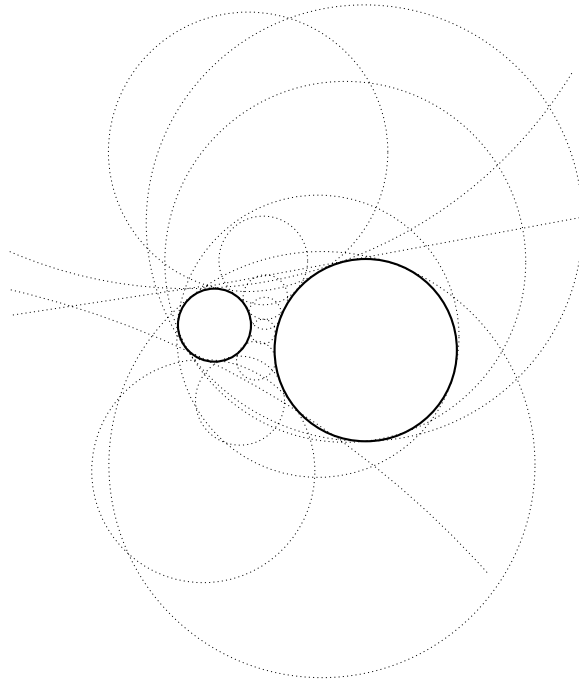


Figure 4.2: Generalized ball-map between two disjoint spheres

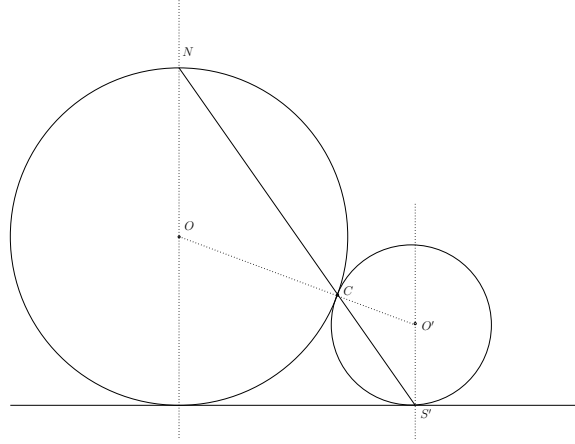


Figure 4.3: The stereographic projection is the ball-map between the sphere and the plane.

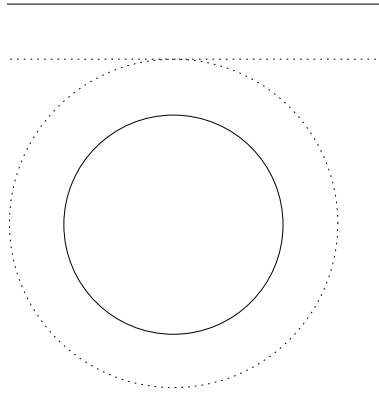


Figure 4.4: Case of a plane an a sphere in general position

point S' (south pole of the small sphere) and the sphere at the “contact point” point C . (C, S') is clearly a generalized ball pair. In order to prove the claim, it suffices to show that S' , C , and N are collinear. O , C , and O' are clearly collinear, therefore the angle $\widehat{O'S'C}$ and \widehat{ONC} are equal. Because the triangles $O'S'C$ and ONC are isosceles, they are homothetic triangles. Therefore, $\widehat{O'S'C}$ and \widehat{ONC} are equal and S' , C , and N are collinear.

It is well known that the stereographic map is conformal. We have proven so far that the ball-map between a sphere and a tangent plane is conformal. If the sphere σ is no longer tangent to the plane π but at distance d for example, see figure 4.4, it is possible to inflate the sphere of $d/2$ (d can be negative) to get a new sphere σ' and translate the plane of $d/2$ to get a plane π' in order to make σ' tangent to π' . The ball-map between σ and π can then be expressed as the composition of a scaling from σ toward σ' , then the conformal ball-map between σ' tangent to π' and then the translation from π' toward π . We have proven so far that the generalized ball-map between a sphere and a plane is conformal. Given two spheres, there exists an inversion that send one sphere on a plane and the other on a sphere. This inversion may be used to reduce the case of

two spheres to the case of a plane and a sphere. \square

4.2 Ball-map and isotopy

In this section we introduce two isotopies from S to S' that “morph” any point $x \in S$ to $\text{BM}_{S,S'}(x) \in S'$.

4.2.1 Broken line morph isotopy

Let us define the map $\pi_S : \text{Me}(S, S') \rightarrow S$ as the projection on S which associates to $y \in \text{Me}(S, S')$ its closest point on S : $\forall z \in S, d(y, z) \geq d(y, \pi_S(y))$. The map $\pi_{S'}$ is defined similarly. It is possible to “parametrize” $\text{Moat}(S, S')$ by $\text{Me}(S, S') \times [-1, 1]$:

$$\mathcal{J}(y, t) = \begin{cases} (1+t)y - t\pi_S(y) & \text{if } t \in [-1, 0], \\ (1-t)y + t\pi_{S'}(y) & \text{if } t \in [0, 1]. \end{cases} \quad (4.1)$$

The map \mathcal{J} is then an isotopy that “morphs” S onto S' , called *broken line morph*.

Notice that under the condition $\text{mfs}(S) > \varepsilon$, $\text{mfs}(S') > \varepsilon$, and $d_H(S, S') < \varepsilon$, one can in fact relax the requirement for S and S' to be connected, because $S^{+\varepsilon}$ has exactly one connected component for each connected component of S and each connected component of $S^{+\varepsilon}$ contains exactly one connected component of S' and theorem 2.1.5 can be applied independently to each pair of respective connected components of S and S' . We have therefore:

Theorem 4.2.1 *Let S and S' be two compact $(n-1)$ -manifolds in R^n with $\varepsilon > 0$ such that $\text{mfs}(S) > \varepsilon$, $\text{mfs}(S') > \varepsilon$, and $d_H(S, S') < \varepsilon$. The broken line morph associated to the ball-pairing $\text{BM}_{S,S'}$ is an isotopy from S to S' .*

The existence of an isotopy from S to S' under the condition of this theorem when $n = 3$ has first been proven in [3]. Theorem 4.2.1 extends the result in arbitrary dimensions and provides an explicit isotopy. This theorem has a consequence on the determination of the isotopy type of a surface from a Hausdorff approximation, for example a set of sampled points. Any given compact set, possibly finite, whose Hausdorff distance to a compact set X is less than $\frac{\varepsilon}{2}$ is called an $(\frac{\varepsilon}{2})$ -Hausdorff approximation of X . Note that if a $(\frac{\varepsilon}{2})$ -Hausdorff approximation of S with $\text{mfs}(S) > \varepsilon$ is given, then the topology and even the isotopy class of the surface is completely determined. Indeed if \tilde{S} is any surface satisfying $\text{mfs}(\tilde{S}) > \varepsilon$ and $d_H(X, \tilde{S}) < \frac{\varepsilon}{2}$, one has $d_H(S, \tilde{S}) \leq d_H(X, S) + d_H(X, \tilde{S})$ and, according to theorem 4.2.1, \tilde{S} is isotopic to S .

4.2.2 Circular arc morph isotopy

In the condition of the previous section, we show that it is possible in fact to follow a circular path between $x \in S$ and $x' = \text{BM}_{S,S'}(x)$. Indeed, if $x' = \text{BM}_{S,S'}(x)$ let us consider $c \in C$ such that $x = \pi_S(c)$ and $x' = \pi_{S'}(c)$. When $x \neq x'$, the triple (x, c, x') is an isosceles triangle and hence defines a unique circular arc going from x to x' , tangent to xc at x and to $x'c$ at x' . If x, c and x' are aligned, then this arc degenerates to a straight line segment. The *circular arc morph* consists then in travelling along this arc of circle (or straight line) with a constant speed.

As in theorem 4.2.1, we relax the requirement that S and S' must be connected.

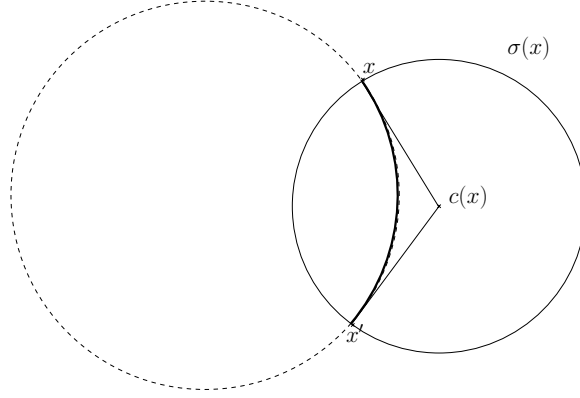


Figure 4.5: The unique circular arc from x to x' , lying inside the ball B_σ , orthogonal to σ at x and x' .

Theorem 4.2.2 *Let S and S' be two compact $(n-1)$ -manifolds in R^n with $\varepsilon > 0$ such that $\text{mfs}(S) > \varepsilon$, $\text{mfs}(S') > \varepsilon$, and $d_H(S, S') < \varepsilon$. The circular arc morph associated to the ball-pairing $\text{BM}_{S, S'}$ is an isotopy from S to S' . Moreover, if S and S' are C^k manifolds, with $k \geq 2$, it defines a C^{k-1} isotopy.*

Proof. — Given a sphere σ bounding a ball B_σ and two points $a \neq b$ on σ , there exists a unique circular arc lying inside B_σ going from a to b being orthogonal to σ at both ends a and b (see fig. 4.5). Indeed if c is the center of σ , it is the unique arc of circle tangent to the isosceles triangle (a, c, b) at a and b .

The continuity of the circular morph in the hypothesis of the theorem follows from the fact that the circular arc depends continuously from the point x, x' and the sphere σ and that both $x' = \text{BM}_{S, S'}(x)$ and σ depend continuously from $x \in S$.

However one has to check that a circular morph defines a one-to-one map between S and intermediate surfaces during the morph (recall that continuous bijections between compact sets are homeomorphisms). We prove in fact the Lemma below which is a stronger result. In the condition of the theorem, let us denote by $\text{Arc}(x)$ the circular (or straight line) segment corresponding to the circular arc morph between x and $x' = \text{BM}_{S, S'}(x)$.

Lemma 4.2.3 *In the condition of the theorem, one has:*

$$\text{Arc}(x) \cap \text{Arc}(y) \neq \emptyset \Rightarrow x = y$$

Proof. — [proof of Lemma 4.2.3]

Let us denote by $x' = \text{BM}_{S, S'}(x)$ the image of x by the ball-map, $\sigma(x)$ the corresponding sphere such that $\sigma(x) \cap S = \{x\}$ and $\sigma(x) \cap S' = \{x'\}$ and $B_{\sigma(x)}$ the closed ball bounded by $\sigma(x)$. Similarly, let us denote by y' , $\sigma(y)$ and $B_{\sigma(y)}$ the point on S' , the sphere and the closed ball corresponding to y . Observe that $\text{Arc}(x) \subset B_{\sigma(x)}$ and $\text{Arc}(y) \subset B_{\sigma(y)}$. Therefore:

$$\text{Arc}(x) \cap \text{Arc}(y) \neq \emptyset \Rightarrow B_{\sigma(x)} \cap B_{\sigma(y)} \neq \emptyset$$

The radical plane $\Pi_{\sigma(x), \sigma(y)}$ of $\sigma(x)$ and $\sigma(y)$ contains $\sigma(x) \cap \sigma(y)$. Moreover observe that if one denotes by $c(x)$ and $c(y)$ the respective centers of $\sigma(x)$ and $\sigma(y)$, $\text{Arc}(x)$ is

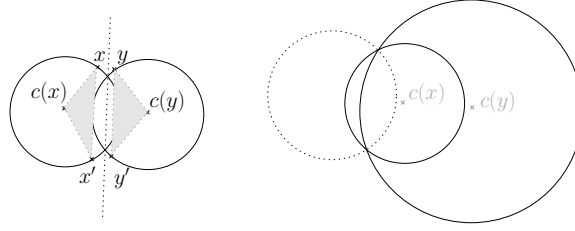


Figure 4.6: On the left, the radical plane $\Pi_{\sigma(x),\sigma(y)}$ of $\sigma(x)$ and $\sigma(y)$ separates the convex hulls of the triples $(x, c(x), x')$ and $(y, c(y), y')$. On the right, the general case is identical to the symmetric case up to an inversion.

in the convex hull of the triple $(x, c(x), x')$ and $\text{Arc}(y)$ is in the convex hull of the triple $(y, c(y), y')$.

Assume, as on the left of figure 4.6, that $\sigma(x)$ and $\sigma(y)$ have same radius, which corresponds to the particular situation where both spheres are symmetric with respect to their radical plane. In this case, $c(x)$ and $c(y)$ lie on opposite sides of the radical plane $\Pi_{\sigma(x),\sigma(y)}$.

We first prove the property in this special case and, in a second step, we prove that any case can be reduced to this particular case by applying an inversion.

Assuming $x \neq y$, because $\text{BM}_{S,S'}$ is one-to-one, one has $x' \neq y'$ and $\sigma(x) \neq \sigma(y)$, and $c(x)$ and $c(y)$ are in opposite open half spaces bounded by $\Pi_{\sigma(x),\sigma(y)}$. Because $\sigma(x) \cap S = \{x\}$, $\sigma(x) \cap S' = \{x'\}$, $\sigma(y) \cap S = \{y\}$ and $\sigma(y) \cap S' = \{y'\}$, one has $x, x' \notin B_{\sigma(y)}$ and $y, y' \notin B_{\sigma(x)}$. Therefore, x and x' lie in the same open half-space bounded by $\Pi_{\sigma(x),\sigma(y)}$ than $c(x)$ and y and y' lies in the same open half-space bounded by $\Pi_{\sigma(x),\sigma(y)}$ than $c(y)$. Therefore the respective convex hulls of $(x, c(x), x')$ and $(y, c(y), y')$ are separated by $\Pi_{\sigma(x),\sigma(y)}$ and $\text{Arc}(x)$ and $\text{Arc}(y)$ cannot possibly intersect.

Let us assume now, as on the right of figure 4.6, that $c(x)$ and $c(y)$ lie on the same side of the plane $\Pi_{\sigma(x),\sigma(y)}$. Notice that, from the unicity of the circular arc defined by a sphere σ and two points $a \neq b$ on σ and because inversions preserve arc of circles as well as local orthogonality, the circular arc defined by $\sigma(x)$ and $x \neq x'$ on $\sigma(x)$ is conformally invariant in the following sense. If I is an inversion with center outside $\sigma(x)$, the circular arc corresponding to the points $I(x)$, $I(x')$ lying on $I(\sigma(x))$ is the image by I of the circular arc corresponding to the points x, x' and the sphere $\sigma(x)$.

It is easy to apply an inversion I with respect to a center outside both $B_{\sigma(x)}$ and $B_{\sigma(y)}$ such that $I(\sigma(x))$ and $I(\sigma(y))$ have the same radius. Therefore, the above mentioned conformal invariance allows to reduce the general situation to the previously considered particular case where both spheres have same radius. \square

\square

Chapter 5

Anticipated applications

We anticipate several possible applications of the ball-map. For example, the ball-map may be used to transfer parameterizations and texture maps [25] between two ball-compatible surfaces (Fig 5.1). Note that it is distortion-free when mapping a planar portion of S to a planar portion of S' (Fig 5.2).

It may also be used to compare two curves or two surfaces. Arguably, measuring the maximum, average, or mean square of the distances between all points x of S and their ball-image $\text{BM}_{S,S'}(x)$ on S' may be more useful than measuring the Hausdorff distance between S and S' .

The isotopies induced by the ball-map may be used to define a morph between S and S' . We propose three possible trajectories for each point x of S to the corresponding point x' of S' : (1) linear interpolation from x to x' , (2) a two-line-segment interpolation from x -to- $c(x)$ -to- x' , and (3) a circular arc that starts at x in the normal direction to S and arrives at x' in the normal direction to S' (Fig. 1.1). The distortions they produce on the texture transferred from the initial surface onto the animated one are compared in the accompanying video.

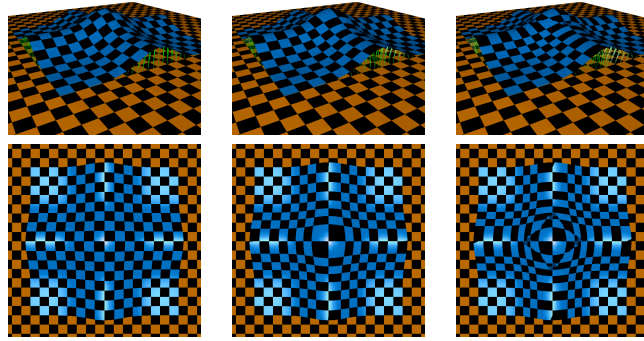


Figure 5.1: The checkerboard texture of the horizontal plane S is mapped onto the curved surface S' in three ways. Left: a point x' of S' inherits the color of the closest point x of S . Center, a point x' of S' inherits the color of the point $\text{BM}_{S',S}(x')$ on S . Right, a point x of S transfers its texture to the closest point x' on S' . The bottom row shows a top view.

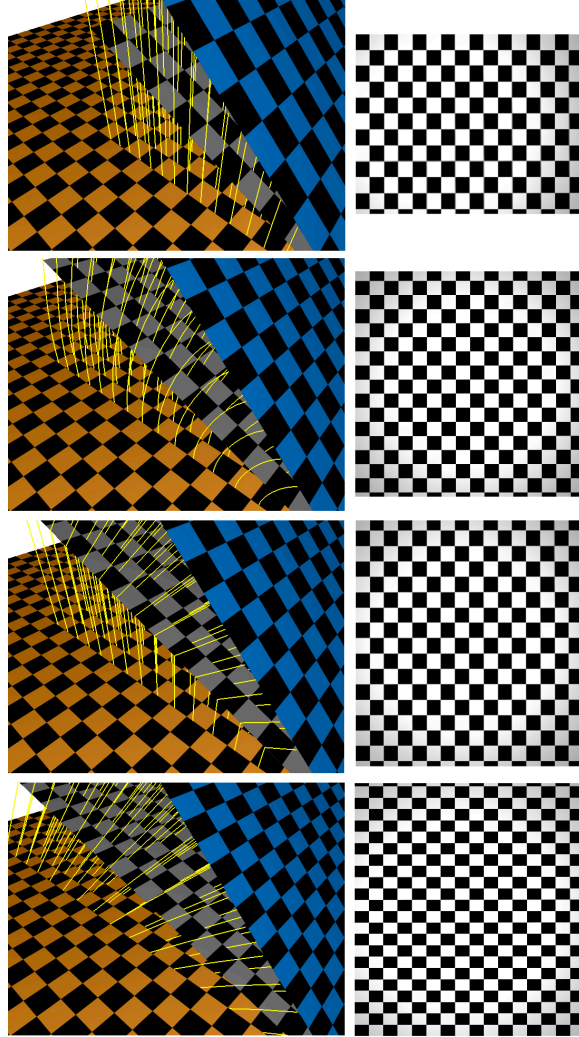


Figure 5.2: The horizontal plane S with its checkerboard texture is morphed onto the slanted plane S' in four different ways. Top-left, a point x of S travels vertically. Top-right, x follows the circular arc defined by the ball-map. Bottom-left, x moves vertically to the median and then to the closest point on S' . Bottom right, x travels to the closest point on S' . We also show the texture on the animated surface mid-course through the morph.

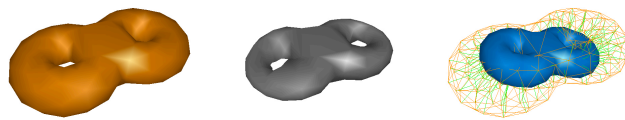


Figure 5.3: The double-torus S (left) is morphed into the smaller double-torus S' (right), positioned partly inside S_i . Broken-lines, x -to- $c(x)$ -to- x' , defined by the ball-map are shown in green (right) along with a wireframe of S . The mid-time frame of the morph is shown (center).

Chapter 6

Conclusion

We introduce the concept of ball-compatible manifolds and show that, when the Hausdorff distance between S and S' is strictly smaller than $\text{mfs}(S)$ and $\text{mfs}(S')$, S and S' are ball-compatible. We introduce the ball-map between two ball-compatible manifolds and show that it is a homeomorphism (theorem 2.1.1). Note that this is a weaker constraint than the one proposed in [8] ensuring that the orthomap is a bijection. For example, if the Hausdorff distance h is 0.8mfs , the ball-map is bijective, but the orthomap may not be. The ball-map may be used to transfer parameterizations, textures, and other properties and annotations between two curves or between two surfaces.

We also prove several smoothness results. In particular, when S and S' are C^k manifolds, then their ball-map is a C^{k-1} diffeomorphism and their median $\text{Me}(S, S')$ is a C^k manifold. We also show that a morph defined by the ball-map is a C^{k-1} isotopy.

Finally, we show that a circular arc may be constructed between x and x' that is orthogonal to S at x and to S' at x' . A morph defined by this circular trajectory for each point x of S eliminates parameterization distortions between planar sections of S and S' and produces visually more pleasing 3D morphs and texture transfers than other mappings, as shown in the accompanying videos.

Bibliography

- [1] M. Alexa. Merging polyhedral shapes with scattered features. *The Visual Computer*, 16:26–37, 2000.
- [2] M. Berger. *Geometry I*. Universitext Series, Springer Verlag, 1998.
- [3] F. Chazal and D. Cohen-Steiner. A condition for isotopic approximation. In *proc. ACM Symp. Solid Modeling and Applications*. ACM, ACM Press, 2004.
- [4] F. Chazal and A. Lieutier. The "lambda-medial axis". *Graphical Models*, 67(4):304–331, 2005.
- [5] F.H. Clarke. *Optimization and NonSmooth Analysis*. Wiley-Interscience, Kluwer Academic, 1983.
- [6] J. Cohen D. Luebke, M. Reddy, A. Varshney, B. Watson, and R. Hubner. *Levels of Detail for 3D Graphics*. Morgan Kaufmann, 2002.
- [7] J. Dixmier. *General Topology*. Springer Verlag, 1984.
- [8] A. Lieutier F. Chazal and J. Rossignac. Projection-homeomorphic surfaces. In *Symposium on Solid and Physical Modeling*, pages 9–14, Boston, 2005.
- [9] M. Floater. Parametrization and smooth approximation of surface triangulations. *Computer Aided Geometric Design*, 14/3:231–250, 1997.
- [10] A. Hatcher. *Algebraic Topology*. Cambridge University Press, 2002.
- [11] M. Hirsch. *Differential Topology*. Springer Verlag, 2003.
- [12] W. Swelden I. Guskov, K. Vidimce and P. Schroeder. Normal meshes. *SIG-GRAPH'2000 Conference Proc.*, pages 95–102, 2000.
- [13] E. Praun J. Schreiner, A. Asirvatham and H. Hoppe. Inter-surface mapping. *ACM Transactions on Graphics*, 23/3:870–877, 2004.
- [14] Mason J. Williams, J. Rossignac. Morphological simplification. Technical Report GIT-GVU-04-05, Georgia Tech ,GVU Tech. Report GIT-GVU-04-05 (Mason2.pdf), 2005.
- [15] A. Kaul and J. Rossignac. Solid-interpolating deformations: Construction and animation of pips. *Computers Graphics*, 16/1:107–115, 1992.
- [16] A. Lieutier. Any open bounded subset of r^n has the same homotopy type as its medial axis. *Computer-Aided Design*, 36:1029–1046, 2004.

- [17] T. Dey N. Amenta, S. Choi and N. Leekha. A simple algorithm for homeomorphic surface reconstruction. *International Journal of Computational Geometry and Applications*, 12(3):127–153, 2002.
- [18] C. Rocchini P. Cignoni and R. Scopigno. Metro: measuring error on simplified surfaces. *Proc. Eurographics '98*, 17/2:107–115, 1992.
- [19] J. Rossignac. Blending and offsetting solid models. *PhD Dissertation, Electrical Engineering Department, University of Rochester, NY*, 1985.
- [20] J. Rossignac. Education-driven research in cad. *Computer-Aided Design Journal (CAD)*, 36/14:1461–1469, 2004.
- [21] J. Rossignac. Surface simplification and 3d geometry compression. *Chapter 54 in the Handbook of Discrete and Computational Geometry (second edition)*, J. E. Goodman and J. O'Rourke Eds., CRC Press:1209–1240, 2004.
- [22] J. Rossignac and A. Requicha. Constant-radius blending in solid modeling. *ASME Computers In Mechanical Engineering (CIME)*, 3:65–73, 1984.
- [23] J. Rossignac and A. Requicha. Offsetting operations in solid modelling. *Computer-Aided Geometric Design*, 3:129–148, 1986.
- [24] J. Rossignac and A. Requicha. Piecewise-circular curves for geometric modeling. *IBM Journal of Research and Development*, 13:296–313, 1987.
- [25] A. Tannenbaum S. Haker, S. Angenent, R. Kikinis, G. Sapiro, and M. Halle. Conformal surface parameterization for texture mapping. *IEEE Transactions on Visualization and Computer Graphics*, 6/2:181–189, 2000.
- [26] A. Safonova and J. Rossignac. Compressed piecewise circular approximation of 3d curves. *Computer-Aided Design (CAD)*, 35/6:533–547, 2003.
- [27] M. Spivak. *A Comprehensive Introduction to Differential Geometry, Vol. I*. Cloth Bound, 1999.
- [28] A. Sheffer V. Kraevoy and C. Gotsman. Matchmaker: constructing constrained texture maps. *ACM Transactions on Graphics (TOG)*, 21/4:326–333, 2003.